Text to Stealthy Adversarial Face Masks

Ben Lewis *Ben.Lewis@warwick.ac.uk*
Department of Computer Science, University of Warwick

Thomas Moyse
Department of Computer Science, University of Warwick

James Parkinson
Department of Computer Science, University of Warwick

Elizabeth Telford
Department of Computer Science, University of Warwick

Callum Whitfield
Department of Computer Science, University of Warwick

Ranko Lazić *R.S.Lazic@warwick.ac.uk*
Department of Computer Science, University of Warwick

Reviewed on OpenReview: *https://openreview.net/forum?id=XYqCx026AI*

Abstract

Recent studies have demonstrated that modern facial recognition systems, which are based on deep neural networks, are vulnerable to adversarial attacks, including the use of accessories, makeup patterns, or precision lighting. However, developing attacks that are both robust (resilient to changes in viewing angles and environmental conditions) and stealthy (do not attract suspicion by, for example, incorporating obvious facial features) remains a significant challenge. In this context, we introduce a novel diffusion-based method (DAFR) capable of generating robust and stealthy face masks for dodging recognition systems (where the system fails to identify the attacker). Specifically our approach is capable of producing high-fidelity printable textures using the guidance of textual prompts to determine the style. This method can also be adapted for impersonation purposes, where the system misidentifies the attacker as a specific other individual. Finally, we address a gap in the existing literature by presenting a comprehensive benchmark (FAAB) for evaluating adversarial accessories in three dimensions, assessing their robustness and stealthiness.

1 Introduction

Facial recognition systems have increasing prominence, with applications in a range of environments. Importantly, these systems aim to accurately classify an individual when presented with an image of them, hence, adversarial attacks against such systems are important to identify and explore. Deep learning facial recognition systems, the state of the art technique for biometric identification (Vakhshiteh et al., 2021), have a history of said attacks, causing the systems to behave in an unintended manner when presented with images that have been carefully modified by attacks.

Previous studies on the matter have used a plethora of both attack surfaces and techniques to misdirect these systems into misclassifying individuals. Some explore attacks by digitally perturbing images of faces (Lin et al., 2023), whilst others use makeup (Yin et al., 2021; Sun et al., 2024) or accessories (Sharif et al., 2019; Komkov & Petiushko, 2021; Zolfi et al., 2022; Gong et al., 2024; Pautov et al., 2019; Xiao et al., 2021). Traditionally, gradient descent based approaches have been employed to generate accessories, to much success

(Zolfi et al., 2022); however, whilst these achieve robustness to changes in viewing angles and environmental conditions, they lack in stealthiness – the need for the attacks to be undetectable by human observers.

Many developments have been made to this regard in order to balance the adversarial strength of an attack with the style and realism of the perturbations. Various loss functions have been explored such as total variation loss (Mahendran & Vedaldi, 2015) which makes the perturbations smoother, making an attack more stable, realistic and robust to interpolation techniques (Komkov & Petiushko, 2021; Zolfi et al., 2022). Other work has used style extractors, L1 losses with a reference style, to make a style adapt to an attack in order to encourage the generation of a stealthy accessory that would not raise suspicion in the real world (Gong et al., 2024). A common struggle with these approaches is generating perturbations that look stealthy consistently, especially against larger facial recognition models such as those based on ResNet (He et al., 2016). When attacks are not attempting to maximize stealthiness, the final perturbations often contain facial features and noise-like perturbations. On the other hand, when attacks prioritize stealthiness, their efficacy is significantly reduced.

Recent literature for general adversarial attacks have propagated towards the use of generative models to support the generation of realistic adversarial examples and perturbations. These methods use a pretrained model to produce or manipulate an adversarial sample towards a given style. Song et al. (2018) used generative adversarial networks (GANs) to generate significantly more realistic examples than were possible with perturbation based methods. Alternatively, diffusion models have too been shown to support generation of adversarial samples (Xue et al., 2023; Chen et al., 2023; Dai et al., 2024) and have several desirable properties for this task, such as greater interpretability, controllability and visual fidelity in the produced samples (Dai et al., 2024).

Diffusion models have been used to generate adversarial makeup (Sun et al., 2024), but to the best of our knowledge, there has been no work on their use in the creation of adversarial accessories. Since the COVID-19 pandemic, the use of face masks by the general public has increased and makes them a prime adversarial accessory surface as they cover a substantial area of the face (Zolfi et al., 2022; Gong et al., 2024).

Figure 1: Adversarial DAFR masks against MobileFaceNet for "David Beckham", "George Clooney" "Angelina Jolie" from the PubFig dataset (Kumar et al., 2009).

By using adversarial guidance (Dai et al., 2024) during the generative process and text prompts to control the style, adversarial optimization and style generation can happen simultaneously, allowing the adversarial perturbations to become part of the style content and leading to truly stealthy and robust adversarial face masks. To this end, we propose the resulting diffusion-based face mask attack that we call Diffusion Attack against Facial Recognition (DAFR) that is able to achieve state of the art stealthiness in a white-box threat model, where the attacker has access to the victim model's weights. In addition to a new novel attack, we propose a benchmark to tackle the current inconsistent experimental frameworks and results within the field, largely caused by varying threat models and attack objectives. This system, titled the Face Accessory Attack Benchmark (FAAB), has been designed with flexibility at its core, allowing it to be adapted to a wide range of attack objectives, so that more consistent evaluation and comparison of attack methods can be performed, focusing on robustness to different conditions, stealthiness and adversarial strength.

In summary, our main contributions are:

- A novel diffusion-based stealthy adversarial face mask generation method, titled DAFR, which uses adversarial guidance to produce adversarial textures that retain the content of the reference images and that can be styled using text prompts. The resulting generated face masks are stealthy, robust to environmental changes, and comparable to previous work.
- A robust benchmarking framework, called FAAB, that includes a set of standardized tests and procedures to evaluate the performance of accessories. The framework supports frequently used statistics like cosine distances, success rates, and a new metric that we discuss later that is based on CMMD, in order to

evaluate the stealthiness of generated textures quantitatively. In addition, the modular design of the benchmark allows each component to be easily interchanged in order to suit each attack's objective.

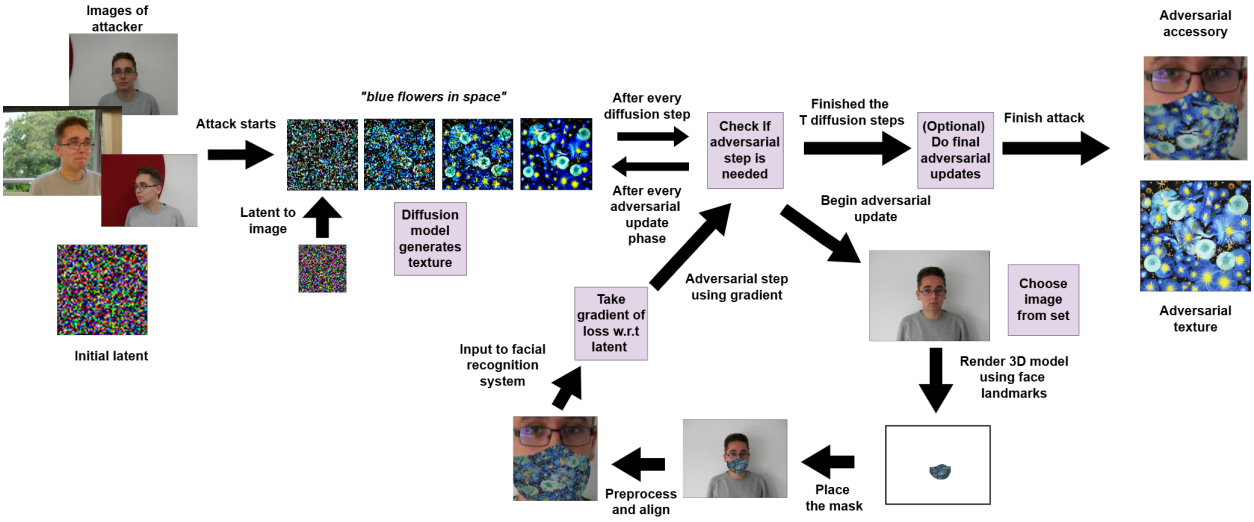

Figure 2: A diagram of the framework of DAFR. Given a text prompt and a set of images of the attacker, DAFR iteratively optimizes the face mask texture to be adversarial over multiple diffusion steps. A differentiable renderer is used to apply the face mask texture to an image of a face which is then back-propagated through to obtain the gradient used in adversarial steps. Each adversarial step uses the gradient of applying the current face mask to a different image to improve the robustness to real life conditions, with multiple adversarial steps performed every diffusion step. Entangling style and adversarial generation allows for the both directions to collaborate to create stealthy adversarial face masks with the visual fidelity of diffusion models. Note that the rendering of the accessory may look different based on the adversarial attack and the rendering shown here is from a differentiable rendering pipeline we developed, but is not used in the evaluation in this work.

2 DAFR: Diffusion Attack against Facial Recognition

Facial Recognition: Modern facial recognition networks are often Siamese networks (Bromley et al., 1993) that are designed to work with a large number of classes and with potentially unseen identities during testing (Wen et al., 2016). These models can be split into two components: the backbone and head. The backbone takes in an image and outputs the embedding of that image in the learnt feature space, which can then be fed into a head for final classification. The embedding spaces are trained to be discriminative and to be effective for multiple different heads for different recognition problems. Recent adversarial work focuses on attacking the backbone directly rather than the head (Vakhshiteh et al., 2021; Zolfi et al., 2022; Gong et al., 2024) and we follow suit. A further discussion of facial recognition systems can be found in appendix A.

Preliminaries: The objective of DAFR is to produce textures for face masks that are not only adversarial to a target network with a backbone, E, but stealthy as well. To do this, the reverse diffusion process of a diffusion model can be manipulated such that the final output looks like the output if the reverse process was not manipulated (i.e, is stealthy) and is adversarial.

One way to control the generation of a diffusion model is classifier guidance where the scores (the gradient of the log of a function) of a classifier are used during generation to perform conditional generation (Dhariwal & Nichol, 2021). AdvDiff is a recent diffusion-based adversarial attack that uses adversarial guidance (Dai et al., 2024), based on classifier guidance, to control the generation of a class conditional latent diffusion model (LDM, Rombach et al. (2022)) to generate unrestricted adversarial examples for ImageNet (Deng et al., 2009).

To achieve this they perform a single adversarial guidance step to the last few diffusion steps during generation to generate an adversarial example and then it uses the current example to optimizes the original latent to become more adversarial. This creates an iterative process where they run the diffusion process then optimize the original latent iteratively to generate stronger adversarial samples. The original AdvDiff attack for dodging optimizes x and z such that for a given label, y, and classifier, where g returns the top label from a given input, then generated samples are in the following set:

$$A_{UAE} = \{x \in G(z, y) | y \neq g(x)\}$$

The above formulation is not compatible with facial recognition systems. Firstly, they are often Siamese based and the recognition threshold may be unknown. For a texture to be adversarial, it must have a low cosine similarity with the anchor embedding, e_a, of the attacker and preferably be under a recognition threshold such that the network would not recognize the masked image as the attacker, this is called *dodging*. If the similarity is maximized with the anchor of a specific other identity, then it is called *impersonation*. We focus on dodging, but our attack can be adapted for impersonation too.

Secondly, it is well documented that adversarial patches (and thus adversarial accessories too) must consider different real world transformations during generation so that the resulting accessories would exhibit robustness to these transformations when they do occur (Athalye et al., 2018). Therefore, to generate physically realizable 3D masks that can be applied to multiple images, the generated textures must be rendered onto a diverse set of face images, H, of the attacker using a rendering function, R. This ensures that the mask is optimized over a diverse range of conditions, such as varying face poses and backgrounds, and will be more applicable to a wider range of real world conditions.

Face masks only cover part of the full input into the network and are worn in different conditions, with the pose of the face and lighting conditions changing how the texture is applied to the input dramatically. This creates a difficult optimization problem where given a set of pictures of the attacker in H we optimize the face mask texture x to minimize the problem below, where *cos* is the cosine similarity.

$$\arg\min_{x} \sum_{h \in H} cos(E(R(x, h)), e_a)$$

A similar optimization problem has been tackled in Zolfi et al. (2022) and Gong et al. (2024). Zolfi et al. (2022) first used differentiable rendering to use gradient methods to generate face mask textures that are adversarial. Gong et al. (2024) built on this to generate mask that were stealthy and adversarial by using an adaptive style generation technique which chooses the best possible style from a given set then optimizes it further for adversarial strength. Both pieces of work optimize over a set of images to ensure that the generated masks are robust to diverse range of conditions,

DAFR: We fuse together adversarial guidance within diffusion and 3D rendering to allow for a more advanced procedure to generate samples that can act as textures for stealthy adversarial masks, as demonstrated in algorithm 1. Since we use LDM's, adversarial guidance is applied to latents, not on the pixel level. f is defined in equation (1).

Figure 3: The left image is a generated texture, the middle is the UV mask and the right is a processed mask texture. We refer to the leftmost image as the texture image and a cropped version of the rightmost image (figure 5) as the masked texture image.

One of the first challenges faced when designing DAFR was adding the flexibility in style desired for a stealthy mask. For this, we chose to use text-to-image models, rather than class conditional models, to condition the generation of samples such that the style is dictated by a text prompt. Classifier free sampling (Ho & Salimans, 2022) is the dominant method for conditioning generation and can be used in conjunction with the guidance, allowing for the generation to achieve both goals.

Additionally, a 3D differentiable rendering pipeline is used so that the texture could not only be rendered onto a 3D face mask, but also have gradients from the target network backpropagate through it. Zolfi et al.

Algorithm 1: Diffusion Attack on Facial Recognition (DAFR)

Input: set of attacker pictures (H), text prompt (c), dodging sign (d), anchor embedding (e_a), adversarial limit (l), iterations of the adversarial loop (k), adversarial guidance weight (s), facial recognition backbone (E), generation timesteps (T)

$x_T \sim \mathcal{N}(0, \mathbf{I})$
for t from T to *1* **do**
  Sample x_{t-1} using classifier free sampling, using x_t and c
  if $t/T \leq l$ **then**
    for i from *1* to k **do**
      h_n = Next image in H
      // d should be -1 if dodging and +1 if impersonating
      $x_{t-1} = x_{t-1} + ds \cdot f(t/T) \cdot \nabla_{x_{t-1}} \cos(E(R(x_{t-1}, h_n)), e_a)$
return x_0

(2022) developed such a pipeline as long as the texture could be fit into a 2D UV mask, shown in figure 3, which we use in this work. We find that optimal performance occurs when the texture is resized to fit most of the content within the UV mask, allowing the perturbation to manifest across a large area of the latent sample.

Generating images that follow text prompts that are also adversarial to facial recognition networks is more abstract (and thus more challenging) than generating samples that use class conditionals of the target network to make it look like another one of the classes – this is without considering the challenges relating to the generated image being a texture applied to a variety of different images, rather than being the final example itself with no concerns for any other image. By optimizing for multiple distinct images, the aim is so that when the texture is applied to a mask on an unknown image, the mask will be robust to environmental conditions and remain adversarial. Optimizing over a single image is significantly easier, but will generate a texture that is not robust to different environmental changes.

This led to the introduction of multiple mechanisms to control the adversarial elements of generation which emphasize different aspects of texture generation:

1. We introduce an inner loop which **increases the number of step of adversarial guidance done per time step** (controlled by k in algorithm 1). By turning each diffusion step into an iterative adversarial process rather than a single step, we are able to find stronger adversarial perturbations similar in fashion to PGD (Madry et al., 2018) tending to generate stronger perturbations than FGSM (Goodfellow et al., 2015). Stronger adversarial perturbations are required compared to the original AdvDiff attack (Dai et al., 2024) because DAFR is not able to optimize the entirety of the input to the network. Due to the face mask being applied to new images, these uncontrolled areas will also change and the part we can control will change and transform between images thus requiring a stronger perturbation. Having a sufficient number of adversarial steps is important due to the importance of optimizing the texture to work over different images.

2. We introduce a hyperparameter to control **how early in the reverse process we begin adversarial guidance** (controlled by l in algorithm 1) which allows for more adversarial steps. However, as demonstrated by Du et al. (2023) the early stages of the diffusion schedule generate coarse structures that have a significant impact on the rest of the generation so one must be careful. Carelessly adding perturbations in the earlier stages of generation can negate the generation of the style while adding in the later stages can result in the perturbation clashing with the style and creating visible perturbations. By adding this as a hyperparameter, this enables to further control the tradeoff between stealth and adversarial strength.

3. DDIM sampling (Song et al., 2021) is used which allows for a **variable number of sampling steps** in the time schedule (controlled by T in algorithm 1). More steps could spread the generation over multiple steps allowing for the adversarial perturbation to slowly coalesce into the style content.

4. The **step size** of each adversarial step (controlled by s in algorithm 1) can be changed to influence generation.

The above mechanisms most be controlled carefully while trying to achieve both adversarial strength, robustness to real world conditions and stealth. Table 3 and figure 5 demonstrates that changes in the hyperparameters of DAFR can have a significant visual impact on the final texture and that this can manifest differently across different victim models or styles (further shown in appendix C).

We find that a constant step size throughout the entire generation leads to adverse perturbations in the later steps of generation, where the adversarial perturbations significantly override the generated content. We introduce a scaling function in equation (1) to slowly decrease the step size based on the proportion of the time schedule left.

$$f(y) = e^{3(y-0.6)-3\min(0,y-0.5)}, \quad y \in [0,1] \tag{1}$$

Several rounds of refining this equation were required, as initially we used the variance of the noise at each diffusion step, but found that using equation (1) was more effective, potentially due to the adversarial updates in the later time steps not being scaled to be very small.

When DAFR is fully deployed, the final result is shown in figure 1. Compared to previous work (Zolfi et al., 2022; Gong et al., 2024), our masks are significantly stealthier and present new capabilities for these attacks, with respect to the style of generated accessories.

3 Results

Baselines: To evaluate our accessories, we compare them to recent adversarial face mask attacks. Adversarial Mask (Zolfi et al., 2022), shortened to AdvMask for brevity, generates face masks for dodging by using a 3D differentiable pipeline and optimizing the mask to be adversarial while maintaining a low TV loss. SASMask (Gong et al., 2024) generates face masks for impersonation so that given content is included (e.g., flowers); however, uses a style transfer network to change the style to be optimal (e.g., by changing the colour). AdvMask does not attempt to be faithful to a style so we do not report our stealthiness measure for those masks, while SASMask does so we do for them. We also test a white non-adversarial face mask to act as a non-adversarial baseline for comparison.

Datasets: We use two different datasets: PubFig (Kumar et al., 2009), which includes faces of a variety of celebrities, and is where the identities for the dodging benchmark come from, and VGGFACE2-HQ (Chen et al., 2024), which contains GAN upscaled images of the VGGFACE2 dataset (Cao et al., 2018). We randomly choose 100 identities from VGGFACE2-HQ to form part of the finetuned classes and another 900 to be used as part of the threshold selection process.

Target Networks: Vakhshiteh et al. (2021) highlight the lack of diversity in the network types studied; therefore, we test on four different network types using different threat models:

1. **Pretrained Large Recognition Models (R100)**: Large pretrained recognition models are often used in previous work (Zolfi et al., 2022) and are publicly available for anyone to use. We test on the pretrained ArcFace ResNet-100[1] directly, that is, before the finetuning in the FT100 setup. The pretraining was performed on the MS1MV3 dataset (Deng et al., 2019b).

2. **Finetuned Networks (FT100)**: There exists large pretrained backbones that are used for recognition, however, without a head, these networks cannot be used for classification. If a small business wanted to train a recognition network for their employees, then they could do further training on the backbone as well as introducing and training a head. We take a pretrained backbone[1] used in previous work (Zolfi et al., 2022), and perform further training on the 100 identities from VGGFACE2-HQ. This included adding an ArcFace head (Deng et al., 2019a) and training using the Adam optimizer (Kingma & Ba, 2015)

[1]MS1MV3 ResNet-100, available from https://github.com/deepinsight/insightface/blob/master/recognition/arcface_torch/README.md

for 100 epochs, while ensuring to use occlusion as an augmentation method during training to improve performance on masked individuals. The final accuracy on 4,500 test images was 97.15%. Previous work has also targeted finetuned networks (Gong et al., 2024) and by having both finetuned and pretrained networks this highlights the potential effect of finetuning these networks on these attacks.

3. **Facial Representation Encoder (FaRL)**: We test on the image encoder from FaRL (Zheng et al., 2022), a vision transformer (Dosovitskiy et al., 2021) backbone for face analysis tasks, including recognition. We specifically chose the epoch 16 pretrained backbone, as used by Zheng et al. (2022).

4. **Mobile devices (MFN)**: Mobile devices are common, however, running large networks on them is impossible due to hardware constraints. MobileFaceNet (Chen et al., 2018) is an architecture specifically designed for face recognition and verification on mobile and embedded devices; we test a pretrained MobileFaceNet using weights provided by Sun et al. (2024).

Generating stealthy adversarial accessories is a serious threat to the integrity of these models, however the difficulty of this task varies dramatically even in a white box setting (as shown in table 3). By testing a variety of different threat models and types of models, we assess the feasibility and threat these diffusion based stealthy attacks pose to these different systems. Future work should also evaluate their work against diverse range of systems as we find that the behavior of these attacks can vary significantly as shown in figure 5.

Threshold Selection: Siamese networks do not give a direct classification like traditional classification networks, therefore previous work also use recognition thresholds to provide a sense of attack success rate to otherwise arbitrary cosine similarities (Zolfi et al., 2022; Gong et al., 2024; Komkov & Petiushko, 2021). Previous work has used a mixture of reporting cosine similarities and using success thresholds. We decide to report both and calculate thresholds using unseen images (i.e., not used elsewhere in the work) from the identities chosen from VGGFACE2-HQ.

Table 1: Cosine Similarity thresholds and TPRs of the different networks when achieving a FAR of 0.01, the rate of inter-class pairs which are misclassified as intra-pairs. TPR is the proportion of intra-class pairs that are correctly classified as being the same person.

Network	Class count	Masked		Unmasked	
		Threshold	*TPR*	*Threshold*	*TPR*
FT100	*100*	0.5300	0.7835	0.0817	0.9802
	1000	0.8355	0.1799	0.8394	0.2248
R100	*100*	0.2687	0.8643	0.1788	0.9320
	1000	0.2370	0.8736	0.1757	0.9317
FaRL	*100*	0.7684	0.2457	0.6670	0.4959
	1000	0.7657	0.2202	0.6568	0.4711
MFN	*100*	0.6156	0.3376	0.2912	0.8114
	1000	0.6622	0.2169	0.2845	0.8212

Previous work (Zolfi et al., 2022; Yin et al., 2021) chooses a threshold that obtains a false acceptance rate (FAR) of 0.01 on masked images from 1000 identities, with the images coming from a validation set not used elsewhere. Similarly, we use the mean threshold that achieves a FAR of 0.01 over 10 fold cross validation on masked images from a validation set (with the mask being uniformly chosen between a white, black or blue mask and placed on the face). We calculate separate thresholds for the 100 and 1000 classes chosen from VGGFACE2-HQ. We use the masked thresholds in table 1 throughtout this work, however, for completeness we show the thresholds if unmasked images were used in table 1 as well.

Table 1 also demonstrates the performance of the different target networks. Pretrained backbones have been trained to have a highly discriminative embedding space across a wide range of datasets, rather than a separable one across one dataset. This leads them to perform incredibly well on unseen faces and to have the highest TPR in table 1. FT100 was trained for the 100 class scenario and therefore performs well, but then struggles on 1000 classes. This threat model has not been explicitly explored before (with previous work performing further training on their models (Gong et al., 2024)) and highlights vulnerabilities to these models if deployed recklessly. FaRL is a general purpose face encoding and so has not been explicitly trained for recognition, explaining the lower TPR. On the other hand, MFN has been trained for recognition but we expect its smaller size may limit its performance. Despite this, MFN performs the best out of all the networks tested at not being fooled by the non-adversarial mask when using the 100 class threshold and second best when using the 1000 class threshold, demonstrating that it is still an effective network, shown in table 3.

Benchmark Setup: In the following tests we use our benchmark, FAAB (refer to section 4), to test the dodging capabilities of the different mask generation methods on 30 randomly selected identities from PubFig. Each mask is generated using 25 images of the identity and then tested on 10 other images of that same person. The results are aggregated over all 300 tests and reported. The cosine scores are given in the format: mean ± standard deviation. Success rate is given by a threshold that is defined as the proportion of tested masked images of the attacker that the embedding of the masked image had a cosine similarity less than the threshold. Each architecture has two thresholds, "SR 100" and "SR 1000" for the 100 and 1000 class thresholds respectively from table 1.

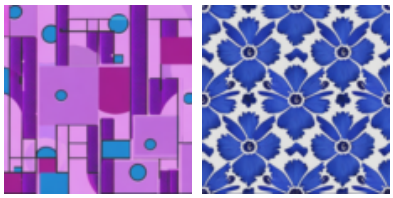

Figure 4: Stealthy masks attempt to be faithful to a reference image. The left image is the reference for purple shapes and the right for blue flowers.

CMMD is performed on the generated texture to measure the stealthiness of an accessory quantitatively (see section 6), but because different attacks use this texture differently in their rendering, we also report CMMD on the final UV 2D mask. Note we use the scaled version of CMMD, with the scale parameters the same as those provided by the authors (Jayasumana et al., 2024).

Table 2: Names and hyperparameter values of different hyperparameter sets for each attack, with DAFR using notation from algorithm 1.

	TV Weight		
AdvMask-a	0.05		
AdvMask-b	0.35		
	Adv. Weight		
SASMask-a	25		
SASMask-b	50		
SASMask-c	600		
SASMask-d	950		
SASMask-e	2000		
	l	s	k
DAFR-a	0.8	7	5
DAFR-b	0.8	7	10
DAFR-c	0.8	10	12
DAFR-d	0.8	2	1

It is important to note that to generate the recognition embedding anchors, we use masked pictures of faces following the procedure of Zolfi et al. (2022) which we now explain. For each identity, 10 unseen images were used for identities from PubFig and 45 images from VGGFACE2-HQ. The mask applied is uniformly chosen from a random noise, white, or black mask. The final anchor embedding is the mean embedding of all the masked images of that identity. Using masked images rather than unmasked images prevents the accessory itself from having a significant impact.

We focus on two different styles for SASMask and DAFR which are advantageous for adversarial masks as an attacker could choose to use any style they want in the real world. The chosen prompts were based on purple shapes[2] and blue flowers[3]. As SASMask uses images as a content reference, the image produced by the diffusion model using the text prompt is used. Figure 4 shows the reference images. Appendix C contains a more complete study of the effect of different styles and text prompts on these attacks.

Implementation Details: MTCNN (Zhang et al., 2016) is used for face alignment with R100, FT100, and FaRL, with FFHQ (Karras et al., 2019) face alignment used for MFN. The differentiable 3D mask rendering pipeline from (Zolfi et al., 2022) is used for placing the masks on faces. The hyperparameters of stealthy mask attacks vary the tradeoff between adversarial strength and stealthiness, therefore we test several sets of hyperparameters which balance this tradeoff. We note that for each DAFR attack, we use 200 DDIM sampling steps. We use Stable Diffusion's v2-1 (Rombach et al., 2022) Text to Image LDM[4] as the diffusion model in DAFR.

We present the results of these attacks with different sets of hyperparameters (as defined in table 2) which allows the main results to act simultaneously as an ablation study. Different hyperparameters present a tradeoff between stealthiness and adversarial strength, with different networks requiring a different hyperparameters to produce effective adversarial attacks. AdvMask only has one hyperparameter which is the weight for the TV loss, for which we test two different values. For SASMask, we keep the style hyperparameters consistent across all sets but change the adversarial weight to be the respective number. The style weights

[2]Prompt: "abstract light purple and pink computer pattern with colorful circles, rectangles, triangles and semi circles like it was made in the 1990s"

[3]Prompt: "blue flower pattern"

[4]Weights for the LDM can be found here.

then are $\lambda_1 = 1000, \lambda_c = 0.01, \lambda_{tv} = 100, \lambda_s = 10000$ using the notation from the original work (Gong et al., 2024). Note that while the original paper does not have an adversarial weight, the official implementation as of writing has always had one. In a practical scenario, an attacker would have to experiment with different hyperparameters to achieve the desired balance between stealth and adversarial efficacy. An attacker could use a surrogate set of images to approximate a recognition threshold which could be used to support finding good hyperparameters.

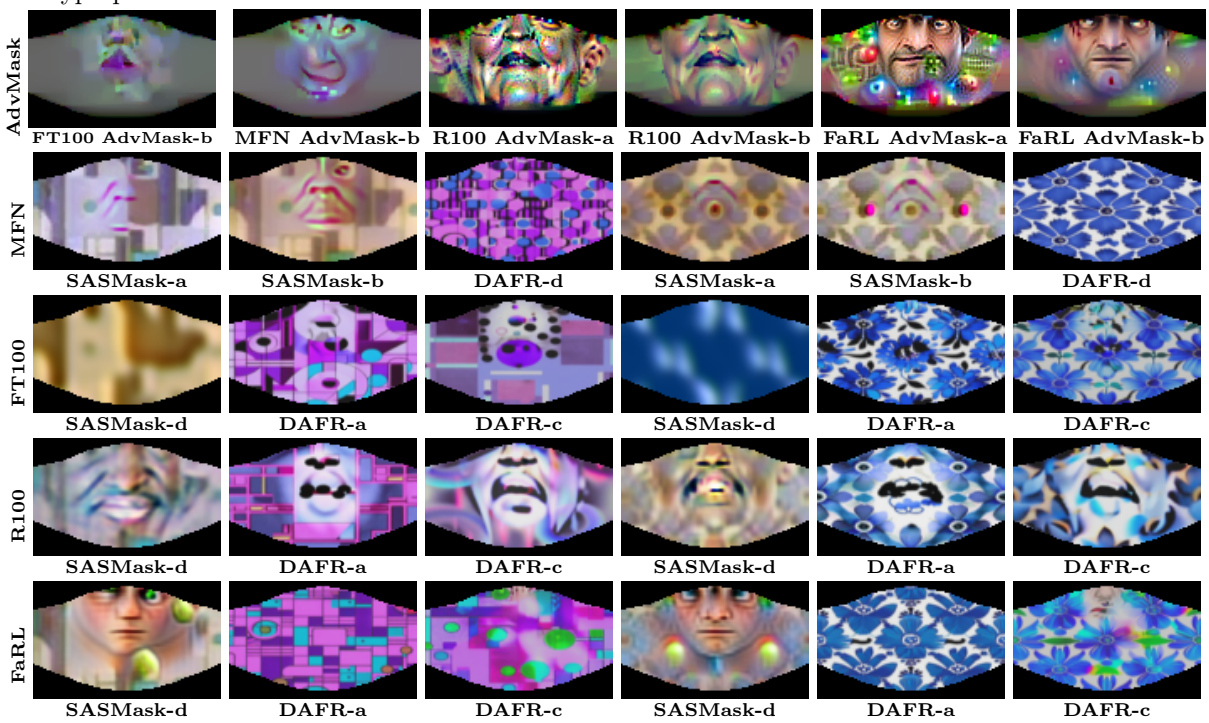

Figure 5: Some of the face mask textures generated as part of the benchmarks within this section for dodging "Beyonce Knowles" in PubFig (Kumar et al., 2009). Underneath each mask is a description of what network it was generated for and the attack used. The top row are all masks generated using the AdvMask attack. For the other rows, the left hand side are generated using the purple shapes style, while the right-hand side are generated using the blue flower style.

Results: The results in table 3 show that DAFR is consistently outperforming previous work in stealthiness, reflected by having a lower M-CMMD than previous stealthy mask attacks, which can be visually confirmed in figure 5. In the majority of cases, especially for FT100 in table 3 and MobileFaceNet in table 3, DAFR has managed to accomplish the dual goal of creating adversarial masks that are effective and stealthy. This is due to the adversarial generation process being able to find adversarial textures that do not deviate substantially from the original generation. We believe this is significant progress as no other work to date has managed to preserve the style and content of a given reference image for adversarial accessories as effectively as ours. This can be seen further in the appendix C where the style generation capabilities are tested further by using wider range of text prompts.

Across all the networks in table 3, we also demonstrate that DAFR can be easily adapted by changing the hyperparameters to balance the tradeoff between stealth and adversarial strength which is reflected in the success rates (SR 100 and SR 1000) and M-CMMD. This flexibility is further reflected in the textures shown in figure 5 where there are significant visual differences between DAFR sets of hyperparameters for the same network and style. Having this flexibility provides practical value, as stealth may be of critical importance in some scenarios.

When attacks do not consider stealthiness (such as AdvMask in table 3), then the adversarial strength of the masks is strong, but still not 100% against some of the networks like FT100 and R100. This demonstrates the challenging threat model of adversarial accessories, where critical facial features for recognition can not

be manipulated, therefore on unseen images it is difficult to cover every possible transformation. Figure 5 presents some of the masks generated by AdvMask which do not achieve a perfect success rate despite focusing on such. One could try to reduce the number of images of the attacker used during generation so that the optimization problem is easier, however this would adversely affect the robustness of these masks to different angles and real world conditions leading to worse real world performance.

Recent work has focused on the architecture of R100 or similar (Zolfi et al., 2022; Gong et al., 2024; Pautov et al., 2019; Komkov & Petiushko, 2021), yet when the same architecture is used but with different weights (such as FT100), the perturbations produced can be drastically different. This is seen in all three attacks tested, suggesting it is not unique to one attack. The masks generated against FaRL also vary dramatically following this trend (see figure 5). One reason this may happen is due to the shape of the gradient output looking like faces, leading to faces being formed in the adversarial generation process with the different attacks handling these faces differently.

The finetuned FT100 was able to achieve the highest TPR on the 100 class problem while achieiving a FAR of 0.01 on unmasked images, refer to table 1. Despite this, FT100 is vulnerable to DAFR's capability to produce very stealthy masks while not sacrificing much adversarial strength compared to AdvMask, as table 3 shows. This should inform real world decisions to avoid reckless use of such technology as it can appear superficially to have an outstanding performance while being incredibly vulnerable to adversaries.

Moreover, FT100 has been trained for a specific 100 class recognition problem rather than the thousands of identities trained for in MS1MV3 (Deng et al., 2019b) leading to a potentially weaker separable embedding space which is not discriminative. Similar face patterns can be seen in other work (Komkov & Petiushko, 2021; Pautov et al., 2019; Zolfi et al., 2022) using the large models from the ICCV 2019 challenge (Deng et al., 2019b). These large models are difficult to fool with stealthy adversarial patches as patches are either adversarial or stealthy with little room in-between. Additionally, there is significant variance between targets (as shown in the standard deviations in table 3) which complicates the problem. Future work should aim to make adversarial masks for these large models while maintaining the visual performance seen on FT100.

4 FAAB: Face Accessory Attack Benchmark

For an adversarial accessory to be considered robust, it is necessary that it is effective in various environmental conditions including lighting, backgrounds and angles. This is not just an important factor during generation, but also when evaluating an accessory's performance. As the results in section 3 demonstrate, the balance between adversarial strength and stealth has a significant impact on the attack success and so it is crucial to evaluate these factors in order to fairly compare approaches.

To date, there is no standardized framework for testing adversarial face accessories (Vakhshiteh et al., 2021), in part due to the varying threat models and attack objectives for work in the field. Whilst benchmarking frameworks exist for neighboring fields, such as GREAT score (Li et al., 2023) for evaluating general adversarial perturbations using generative models, within the realm of adversarial accessories there are inconsistent experimental frameworks that create hard to compare results. Therefore, we propose a highly adaptable benchmarking framework, titled the Face Accessory Attack Benchmark (FAAB), that is capable of consistent and systematic comparison of different attack methods.

To achieve this feat, FAAB uses a systematic procedure for evaluating accessories, with interchangeable components, detailed below:

- **Generation:** an accessory must be generated by the attack being tested for a given individual. It is important at this stage that images used to generate the accessory are not those that will be later used to evaluate, as a strong adversarial accessory should be effective in unseen conditions.
- **Testing:** once the accessory has been generated, the testing phase begins. This consists of loading in dataset images, placing the accessory on the images and computing the output of the recognition system. We calculate statistics based on adversarial strength and the accessory itself, which can be interchanged based on the test. FAAB also keeps track of the performance across different images, such as recording the angle of the face in the images.

Figure 6: Masked face images of "Charlize Theron" and "Jennifer Aniston" using **DAFR-3a** in the benchmark in table 3 on FT100. The variety of poses and backgrounds ensures that during generation and evaluation, masks must be robust to real world transforms.

- **Benchmarking:** to get a holistic view of the performance of an attack method, we repeat the above steps over multiple individuals. To further expand analysis, FAAB supports benchmark variations which can modify how images are augmented such as modifying the brightness of the image. FAAB groups together results based on the properties recorded throughout, such as viewing the performance when the face was at a specific angle. How statistics are grouped is customizable and can help discover links between various properties that have been accumulated in the benchmark.

As alluded to above, it is necessary to quantize how stealthy an accessory is as it is infeasible to construct a manner of evaluating stealthiness through the means of a user survey in such a way as to not introduce bias to one attack and to be fair, especially when the definition of stealthiness itself is often subjective. In section 6 we outline why we believe that CMMD is an effective measure of stealthiness and the resulting values are discussed in section 3. Further principles to evaluating style that could be applied to other work are provided in appendix B.

To demonstrate the robustness of the attacks explored in this paper we analyze the impact of face pose (appendix D), varying brightness (appendix E) and when the mask is applied to images with different lighting on the adversarial mask (appendix F) which is enabled using the FAAB benchmark. Overall, our findings indicate that all the attacks exhibit a level of robustness under varying conditions, suggesting their potential effectiveness in real world scenarios.

5 Physical Evaluation

To validate the efficacy of our attacks in the real world we conducted experiments physically using the authors as the attackers. Photos of each attacker were taken without a face mask to create masked anchors using the same procedure as before. A separate set of 100 photos of each attacker were taken to be used for mask generation for each attack. Some of the adversarial mask textures used for one of the attackers are shown in figure 7 demonstrating that they look aesthetically similar to the masks from the digital tests in figure 5.

The same styles as the digital test were chosen and the hyperparameter sets were chosen based on the digital tests too. Each adversarial texture was then enlarged using cubic interpolation and printed out on paper using a printer resolution of 600 DPI. Small holes were pierced in the left and right of the mask to allow for string to go through allowing for a knot at behind the head to keep the mask up.

Photos were taken in a variety of different lighting conditions, including brightly lit, dim and natural lighting. The person holding the camera moved left to right in front of the attacker with the camera being slightly elevated from the attacker's eyes to ensure that the full face was visible and that the photos were taken from

a diverse range of angles. A Sony A6000 camera was used to take all the photos. Figure 8 illustrates this setup by showing a selection of the photos for one of the attackers.

Before an image can be input into one of the recognition networks it must be aligned to the face which resizes and crops the image to a predetermined perspective the network expects, with the networks used in this work either using MTCNN or FFHQ alignment. To evaluate each attack metric 100 aligned images equally split across the different attackers are used for the networks using MTCNN face alignment. Due to the FFHQ face alignment used on MobileFaceNet not consistently detecting the face when wearing a face mask in the real world, these tests used on average 52 aligned images instead.

Table 4 demonstrates that DAFR is capable to generate physical adversarial masks which are closer to the style while only marginal efficacy when compared to SASMask. SASMask generated masks performed slightly better adversarially than DAFR, however these masks are significantly less stealthy as demonstrated visually in figure 7 and quantitatively in table 3. All the attacks lost some of their efficacy in the physical tests against all the networks compared to their digital counterparts. This could be explained due significantly harder difficulty of the physical evaluations, such as the physical placement not precisely matching the digital placement or the differing lighting conditions affecting the mask.

The cosine similarities on the stronger pretrained R100 and the finetuned FT100 are higher for all three attacks in the physical tests than in the digital tests meaning these networks were particularly more robust physically than digitally. This could be due to many different reasons such as their larger architecture, training specifically for facemasks or many other reason. Future work could look into how these factors affect the robustness of these recognition networks to patch-based adversarial attacks.

6 Related Works

Here we discuss the closest previous works; we comparatively review further literature across several areas in appendix A.

Patch-based Adversarial Attacks on Facial Recognition: Adversarial accessories are small wearables that contain patterns that when placed within an image cause malicious behavior. Previous adversarial accessories have varied significantly in the generation process and in the type of accessory, including glasses (Sharif et al., 2019), hats (Komkov & Petiushko, 2021), face patches (Pautov et al., 2019), eye patches (Xiao et al., 2021) and face masks (Zolfi et al., 2022; Gong et al., 2024). As mentioned in section 1, face masks have seen an increase in usage within the general public and are a prime adversarial accessory as they cover a substantial area of the face (Zolfi et al., 2022; Gong et al., 2024), hence they are our chosen accessory type.

Most adversarial accessory attacks primarily focus on the accessory being adversarial (Sharif et al., 2019; Pautov et al., 2019; Komkov & Petiushko, 2021) or focus on emphasizing additional properties such as transferability (Xiao et al., 2021; Zolfi et al., 2022; Yang et al., 2023; Gong et al., 2024). He et al. (2024) recently generated adversarial face masks that interfere with the entire pipeline of these systems by attacking the face detection, liveness detection and the recognition. However, the generated accessories from these works do not look like "normal" attire and would arouse suspicion if worn in the real world – we would consider these to not be stealthy.

Gong et al. (2024) attempts to explicitly generate stealthy face masks using adaptive styles and style losses, but these cause the texture to depart from a reference image significantly. Concurrent to our work, Xie et al. (2025) generated stealthy masks by using differential evolution to select styles which are both adversarial and stealthy enabling perturbations to occur naturally in the style rather than being perturbed on top of a given style. We focus primarily on stealthiness and argue that for a mask to be stealthy, it must look similar to a reference image. To the best of our knowledge, we are the first to utilize diffusion models to generate adversarial accessories.

Quantitative Measures of Style: Within adversarial attacks on facial recognition, some style measures that have been used before in makeup attacks (Sun et al., 2024) include SSIM (Wang et al., 2004), PSNR and FID (Heusel et al., 2017). Gong et al. (2024) used SSIM in a setup specific to their face mask which is hard to transfer to other attacks. Creating metrics to evaluate the quality of generated images is a problem faced

by generative models and stealthy adversarial accessories that generate textures can be seen as generators that have a baseline style (a "real" set) which can generate multiple adversarial textures (a "generated" set). CLIP Maximum Mean Discrepancy (CMMD) (Jayasumana et al., 2024) is a recent metric proposed to measure the quality of generated images by finding the maximum mean discrepancy (MMD) (Gretton et al., 2006; 2012) between CLIP (Radford et al., 2021) embeddings of a real and generated set of images. An unbiased estimator of MMD on two sets of CLIP embeddings, $X = \{x_1, x_2, ..., x_m\}$ and $Y = \{y_1, y_2, ..., y_n\}$, and kernel k (for which we use a RBF kernel) can be given by the equation below. For the results in this paper, we scaled the output of CMMD for display purposes, using the same values as in the original paper (Jayasumana et al., 2024).

$$dist^2_{MMD}(X, Y) = \frac{1}{m(m-1)} \sum_{i=1}^{m} \sum_{j \neq i}^{m} k(x_i, x_j) + \frac{1}{n(n-1)} \sum_{i=1}^{n} \sum_{j \neq i}^{n} k(y_i, y_j) - \frac{2}{mn} \sum_{i=1}^{m} \sum_{j=1}^{n} k(x_i, y_j)$$

By using CLIP embeddings, CMMD is able to provide a more holistic evaluation of style and previous work has shown CMMD to outperform FID and other common metrics when compared to human raters (Jayasumana et al., 2024) which resonates back to the user surveys in previous accessory work (Sharif et al., 2019). We believe these user surveys for image generation can be further extrapolated to the generation of textures for accessories, thus meaning that CMMD is a good measure of the stealthiness of textures, although future work could confirm this by running human surveys like previous work. Future work should also use CMMD as a metric to evaluate the quality (thus stealthiness) of their generated textures and so having an evaluation that is similar to how image generators are evaluated. More details about how we use CMMD are found in section 4.

7 Conclusion

We propose a novel diffusion-based attack, DAFR, for adversarial mask generation that generates masks that are both adversarial and stealthy. We demonstrate the effectiveness of the attack in both the physical and digital domains on a range of architectures and threat models, and highlight the challenges in attacking these models. Moreover, we propose a robust standardized benchmarking framework, FAAB, for evaluating the strength and stealthiness of these attacks such that comparisons between future work can be quicker, robust, and fair. This further invites future work to use this framework to create strong and stealthy adversarial accessories.

Limitations: We have tested different attacks on a variety of networks and have found that the behavior of the attacks can vary significantly between networks. This unfortunately means that DAFR can struggle to produce stealthy adversarial masks on the strongest networks. Additionally, DAFR uses adversarial guidance (Dai et al., 2024) and is sensitive to the hyperparameters highlighted in table 2. Small changes can lead to significant variation in the output and their values must be adjusted for different target networks. This requires manual testing to balance the stealthiness of the generated mask and its stealthiness.

Future Work: DAFR is substantially better at generating stealthy masks compared to previous work, however there are five main areas for future work to improve upon. *(1)* generating stealthy masks on stronger networks is difficult and future work could expand the number of networks these masks are stealthy for. *(2)* we did not extensively investigate physically realizing the masks within this work and future work could explore whether these masks apply in the real world. *(3)* we propose using new metrics to evaluate stealthiness in the generated textures which previous work has found to align with human perception, future work should run surveys to confirm that these metrics align with human perception when applied to textures on accessories. *(4)* as our work focused on maximizing the stealthiness of the adversarial textures, future work could look at the transferability of these stealthy attacks in a black box setting *(5)* all adversarial face mask attacks are inherently vulnerable to removal by generative based defenses. Given the weights of a face mask removal network, future work could generate masks that are adversarial to the recognition network and the removal network to mitigate this weakness.

FT100, finetuned backbone

Attack	Style	Cosine Sim. (↓)	SR 100 (↑)	SR 1000 (↑)	T-CMMD (↓)	M-CMMD (↓)
Non Adv.	*White*	0.6746 ± 0.2314	0.2767	0.7133	/	/
AdvMask-a	*Random*	0.0380 ± 0.2628	0.9500	0.9800	/	/
AdvMask-b		-0.0128 ± 0.1860	0.9867	1.0000	/	/
SASMask-d	*Purple Shapes*	0.3810 ± 0.3296	0.6200	0.9233	3.1881	1.7600
SASMask-e		0.4541 ± 0.3261	0.5100	0.8800	3.1208	2.0857
DAFR-a		0.2211 ± 0.2314	*0.8900*	**0.9867**	**1.3295**	**0.8471**
DAFR-b		*0.2166 ± 0.2365*	0.8700	0.9733	*1.6960*	*1.1771*
DAFR-c		**0.1816 ± 0.2133**	**0.9167**	*0.9833*	2.3490	1.5018
SASMask-d	*Blue Flowers*	0.4186 ± 0.3731	0.5533	0.8167	3.8306	3.5290
SASMask-e		0.3660 ± 0.3370	0.6600	0.8900	4.0924	2.9544
DAFR-a		0.2306 ± 0.2297	0.8867	*0.9767*	**2.4527**	**1.0090**
DAFR-b		*0.2189 ± 0.2171*	*0.9033*	**0.9900**	*2.8263*	*1.1199*
DAFR-c		**0.1764 ± 0.2232**	**0.9200**	*0.9767*	3.6985	1.6210

MFN, MobileFaceNet

Attack	Style	Cosine Sim. (↓)	SR 100 (↑)	SR 1000 (↑)	T-CMMD (↓)	M-CMMD (↓)
Non Adv.	*White*	0.7303 ± 0.0837	0.1000	0.2100	/	/
AdvMask-a	*Random*	0.3028 ± 0.0871	1.0000	1.0000	/	/
AdvMask-b		0.3496 ± 0.0922	1.0000	1.0000	/	/
SASMask-a	*Purple Shapes*	0.3868 ± 0.1804	0.8633	0.9133	*2.3938*	*1.8368*
SASMask-b		**0.1019 ± 0.1115**	**1.0000**	**1.0000**	3.2128	2.2126
DAFR-d		*0.2874 ± 0.1282*	*0.9967*	**1.0000**	**1.2792**	**0.8416**
SASMask-a	*Blue Flowers*	*0.2549 ± 0.0885*	**1.0000**	**1.0000**	*3.9781*	3.0724
SASMask-b		**0.1471 ± 0.0956**	**1.0000**	**1.0000**	4.1066	*2.9479*
DAFR-d		0.4788 ± 0.0854	0.9533	0.9967	**0.9009**	**0.1040**

R100, pretrained backbone

Attack	Style	Cosine Sim. (↓)	SR 100 (↑)	SR 1000 (↑)	T-CMMD (↓)	M-CMMD (↓)
Non Adv.	*White*	0.6217 ± 0.1921	0.0733	0.0733	/	/
AdvMask-a	*Random*	0.0317 ± 0.1350	0.9500	0.9367	/	/
AdvMask-b		0.0328 ± 0.1287	0.9567	0.9400	/	/
SASMask-c	*Purple Shapes*	**0.1064 ± 0.1279**	**0.9100**	**0.8467**	3.0740	2.5177
SASMask-d		*0.1091 ± 0.1381*	*0.8833*	*0.8200*	3.3451	2.5361
SASMask-e		0.1171 ± 0.1574	0.8533	0.8066	3.4989	2.9703
DAFR-a		0.2546 ± 0.1410	0.5267	0.4267	**1.5728**	**1.2138**
DAFR-b		0.1909 ± 0.1396	0.6900	0.6233	*2.2289*	*1.7903*
DAFR-c		0.1787 ± 0.1436	0.7467	0.6433	3.0438	2.4713
SASMask-c	*Blue Flowers*	0.1077 ± 0.1401	0.8667	0.8300	4.1449	4.5054
SASMask-d		*0.0926 ± 0.1418*	*0.9100*	*0.8667*	4.4332	4.7600
SASMask-e		**0.0803 ± 0.1298**	**0.9233**	**0.8933**	4.5162	3.4040
DAFR-a		0.2678 ± 0.1450	0.4967	0.4233	**2.9012**	**1.2724**
DAFR-b		0.2020 ± 0.1407	0.6733	0.5867	*3.9275*	*1.7545*
DAFR-c		0.1769 ± 0.1448	0.7267	0.6567	4.9682	2.4842

FaRL, pretrained ViT

Attack	Style	Cosine Sim. (↓)	SR 100 (↑)	SR 1000 (↑)	T-CMMD (↓)	M-CMMD (↓)
Non Adv.	*White*	0.8078 ± 0.0584	0.2067	0.1800	/	/
AdvMask-a	*Random*	0.3777 ± 0.0984	1.0000	1.0000	/	/
AdvMask-b		0.4013 ± 0.1043	1.0000	1.0000	/	/
SASMask-d	*Purple Shapes*	**0.4213 ± 0.0997**	**1.0000**	**1.0000**	2.7931	2.6759
SASMask-e		*0.4322 ± 0.1206*	**1.0000**	**1.0000**	2.7984	2.5965
DAFR-a		0.7482 ± 0.0522	0.6367	0.6200	1.5283	0.8031
DAFR-b		0.7333 ± 0.0532	0.7433	0.7167	**1.2023**	**0.9583**
DAFR-c		0.7150 ± 0.0561	0.8333	0.8233	*1.4417*	*0.8877*
SASMask-d	*Blue Flowers*	**0.3787 ± 0.0960**	**1.0000**	**1.0000**	4.9293	3.4139
SASMask-e		*0.3881 ± 0.0954*	**1.0000**	**1.0000**	4.9995	4.8929
DAFR-a		0.7671 ± 0.0503	0.4500	0.4300	**1.7892**	**0.5895**
DAFR-b		0.7565 ± 0.0512	0.5433	0.5133	*2.4341*	*1.0099*
DAFR-c		0.7258 ± 0.0544	0.8033	0.7900	3.0446	1.1998

Table 3: Results of the four dodging benchmarks of the different networks tested, as outlined in section 3. The first set of columns indicate the attack and its style, the second set of columns indicate the attack statistics aggregated over the 300 test images in each benchmark when the targeted attacker wears the mask, and the final set of columns are accessory statistics aggregated over the 30 generated textures.

Arrows next to each column indicate the desired direction of each metric, for example ↓ would indicate lower values are desirable. Cosine similarity is in the format of *Mean* ± *Std-Deviation* over the test images. SR 100 and SR 1000 are the success rate of the dodging masks over the test set using the thresholds in table 1. T-CMMD and M-CMMD are defined as the CMMD (refer to section 6) over the texture images and mask texture images (see figure 3 for the difference). Different attacks convert their texture onto the mask differently therefore M-CMMD is a fairer evaluation. For each column within attacks using the same style, a marker has been used to indicate rank: **1st**, *2nd* and 3rd.

DAFR outperforms SASMask for every network in terms of stealth (shown in the CMMD columns), while either outperforming SASMask adversarially or by sacrificing minimal adversarial strength.

Arch.	Attack	Style	Cosine Sim. (↓)	SR 100 (↑)	SR 1000 (↑)
FT100	***Non Adv.***	*White*	0.8015 ± 0.1765	0.0700	0.4000
	AdvMask-b	*Random*	0.7814 ± 0.1487	0.0800	0.5600
	DAFR-b	*Purple Shapes*	0.7377 ± 0.1243	0.0500	0.7300
	SASMask-d		$\mathbf{0.6705 \pm 0.1485}$	**0.1200**	**0.8900**
	DAFR-b	*Blue flowers*	0.7730 ± 0.1451	0.0900	0.5500
	SASMask-d		$\mathit{0.6979 \pm 0.1385}$	*0.1000*	*0.8100*
MFN	***Non Adv.***	*White*	0.6105 ± 0.1876	0.3333	0.4444
	AdvMask-b	*Random*	0.0793 ± 0.2442	0.9900	0.9900
	DAFR-b	*Purple Shapes*	0.5250 ± 0.1440	0.7000	0.8500
	SASMask-d		$\mathit{0.3406 \pm 0.1846}$	0.8852	*0.9016*
	DAFR-b	*Blue flowers*	0.4906 ± 0.1210	*0.8986*	0.8986
	SASMask-d		$\mathbf{0.2589 \pm 0.1112}$	**0.9700**	**0.9800**
R100	***Non Adv.***	*White*	0.6197 ± 0.1585	0.0500	0.0400
	AdvMask-b	*Random*	0.4716 ± 0.2698	0.3100	0.2800
	DAFR-b	*Purple Shapes*	$\mathit{0.5442 \pm 0.2102}$	0.1300	0.1000
	SASMask-d		$\mathbf{0.2423 \pm 0.2072}$	**0.5700**	**0.5500**
	DAFR-b	*Blue flowers*	0.6299 ± 0.2291	0.1100	0.1100
	SASMask-d		0.5625 ± 0.2443	*0.1900*	*0.1500*
FaRL	***Non Adv.***	*White*	0.7892 ± 0.0475	0.2400	0.2400
	AdvMask-b	*Random*	0.6410 ± 0.0955	0.9500	0.9500
	DAFR-c	*Purple Shapes*	0.7423 ± 0.0328	0.7900	0.7100
	SASMask-d		$\mathit{0.6430 \pm 0.1059}$	*0.8800*	*0.8800*
	DAFR-c	*Blue flowers*	0.7583 ± 0.0289	0.7100	0.6500
	SASMask-d		$\mathbf{0.5712 \pm 0.1079}$	**0.9800**	**0.9900**

Table 4: Physical tests where each test uses 100 images equally split between the attackers for the tests on FT100, R100 and FaRL. In the case of MFN, due to the FFHQ face alignment, the average number of images per test is 52. For each column within the styled attacks on the same target network, a marker has been used to indicate rank: **1st**, *2nd* and 3rd. Whereas figure 7 and table 3 show that DAFR generates adversarial masks that are stealthier and more stylistic, this table shows that DAFR is effective in the physical space too while sacrificing only a marginal amount of efficacy compared to SASMask.

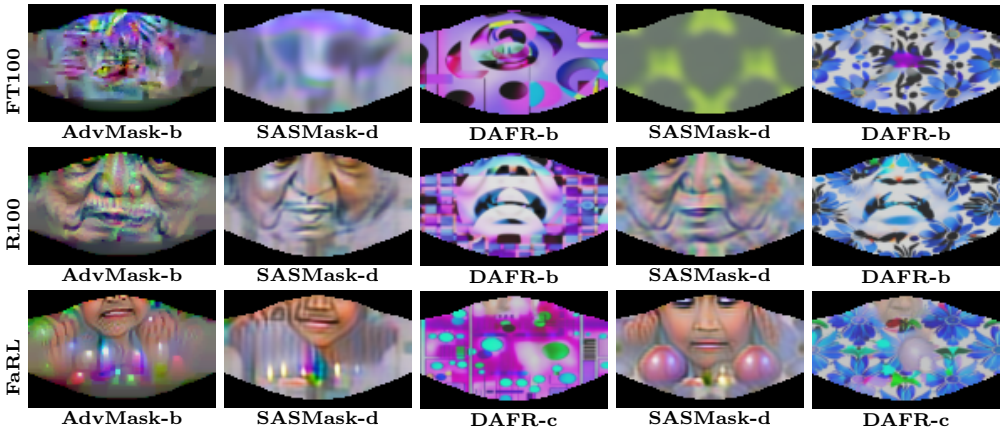

Figure 7: The textures of the masks used during the physical evaluation for one of the attackers. Within each row, the first two styled masks are styled with purple shapes and the latter two are styled with blue flower patterns. DAFR is capable of producing perturbations that are visually consistent with the style enabling for stealthier masks.

Figure 8: A selection of the photos from the physical evaluation tests, demonstrating the variety of different backgrounds, lighting, and angles used. Each pair of columns shows a different background, and each row shows a different mask. Every photo was taken from a slightly elevated position from the eyes.

References

Anish Athalye, Logan Engstrom, Andrew Ilyas, and Kevin Kwok. Synthesizing Robust Adversarial Examples. In *Proceedings of the 35th International Conference on Machine Learning, ICML 2018, Stockholmsmässan, Stockholm, Sweden, July 10-15, 2018*, volume 80 of *Proceedings of Machine Learning Research*, pp. 284–293. PMLR, 2018. 4, 22

Jane Bromley, James W. Bentz, Léon Bottou, Isabelle Guyon, Yann LeCun, Cliff Moore, Eduard Säckinger, and Roopak Shah. Signature Verification Using A "Siamese" Time Delay Neural Network. *Int. J. Pattern Recognit. Artif. Intell.*, 7(4):669–688, 1993. 3, 22

Tom B. Brown, Dandelion Mané, Aurko Roy, Martín Abadi, and Justin Gilmer. Adversarial Patch. *CoRR*, abs/1712.09665, 2017. 22

Qiong Cao, Li Shen, Weidi Xie, Omkar M. Parkhi, and Andrew Zisserman. VGGFace2: A Dataset for Recognising Faces across Pose and Age. In *13th IEEE International Conference on Automatic Face & Gesture Recognition, FG 2018, Xi'an, China, May 15-19, 2018*, pp. 67–74. IEEE Computer Society, 2018. 6

Sheng Chen, Yang Liu, Xiang Gao, and Zhen Han. MobileFaceNets: Efficient CNNs for Accurate Real-Time Face Verification on Mobile Devices. In Jie Zhou, Yunhong Wang, Zhenan Sun, Zhenhong Jia, Jianjiang Feng, Shiguang Shan, Kurban Ubul, and Zhenhua Guo (eds.), *Biometric Recognition - 13th Chinese Conference, CCBR 2018, Urumqi, China, August 11-12, 2018, Proceedings*, volume 10996 of *Lecture Notes in Computer Science*, pp. 428–438. Springer, 2018. 7

Xinquan Chen, Xitong Gao, Juanjuan Zhao, Kejiang Ye, and Cheng-Zhong Xu. AdvDiffuser: Natural Adversarial Example Synthesis with Diffusion Models. In *IEEE/CVF International Conference on Computer Vision, ICCV 2023, Paris, France, October 1-6, 2023*, pp. 4539–4549. IEEE, 2023. 2, 22

Xinyun Chen, Chang Liu, Bo Li, Kimberly Lu, and Dawn Song. Targeted Backdoor Attacks on Deep Learning Systems Using Data Poisoning. *CoRR*, abs/1712.05526, 2017. 23

Xuanhong Chen, Bingbing Ni, Yutian Liu, Naiyuan Liu, Zhilin Zeng, and Hang Wang. SimSwap++: Towards Faster and High-Quality Identity Swapping. *IEEE Trans. Pattern Anal. Mach. Intell.*, 46(1):576–592, 2024. 6

Xuelong Dai, Kaisheng Liang, and Bin Xiao. AdvDiff: Generating Unrestricted Adversarial Examples Using Diffusion Models. In Ales Leonardis, Elisa Ricci, Stefan Roth, Olga Russakovsky, Torsten Sattler, and

Gül Varol (eds.), *Computer Vision - ECCV 2024 - 18th European Conference, Milan, Italy, September 29-October 4, 2024, Proceedings, Part XLVI*, pp. 93–109. Springer, 2024. 2, 3, 5, 13, 22

Jia Deng, Wei Dong, Richard Socher, Li-Jia Li, Kai Li, and Li Fei-Fei. ImageNet: A large-scale hierarchical image database. In *2009 IEEE Computer Society Conference on Computer Vision and Pattern Recognition (CVPR 2009), 20-25 June 2009, Miami, Florida, USA*, pp. 248–255. IEEE Computer Society, 2009. 3

Jiankang Deng, Jia Guo, Niannan Xue, and Stefanos Zafeiriou. ArcFace: Additive Angular Margin Loss for Deep Face Recognition. In *IEEE Conference on Computer Vision and Pattern Recognition, CVPR 2019, Long Beach, CA, USA, June 16-20, 2019*, pp. 4690–4699. Computer Vision Foundation / IEEE, 2019a. 6, 22

Jiankang Deng, Jia Guo, Debing Zhang, Yafeng Deng, Xiangju Lu, and Song Shi. Lightweight Face Recognition Challenge. In *2019 IEEE/CVF International Conference on Computer Vision Workshops, ICCV Workshops 2019, Seoul, Korea (South), October 27-28, 2019*, pp. 2638–2646. IEEE, 2019b. 6, 10

Prafulla Dhariwal and Alexander Quinn Nichol. Diffusion Models Beat GANs on Image Synthesis. In *Advances in Neural Information Processing Systems 34: Annual Conference on Neural Information Processing Systems 2021, NeurIPS 2021, December 6-14, 2021, virtual*, pp. 8780–8794, 2021. 3

Alexey Dosovitskiy, Lucas Beyer, Alexander Kolesnikov, Dirk Weissenborn, Xiaohua Zhai, Thomas Unterthiner, Mostafa Dehghani, Matthias Minderer, Georg Heigold, Sylvain Gelly, Jakob Uszkoreit, and Neil Houlsby. An Image is Worth 16x16 Words: Transformers for Image Recognition at Scale. In *9th International Conference on Learning Representations, ICLR 2021, Virtual Event, Austria, May 3-7, 2021*. OpenReview.net, 2021. 7

Chengbin Du, Yanxi Li, Zhongwei Qiu, and Chang Xu. Stable Diffusion is Unstable. In *Advances in Neural Information Processing Systems 36: Annual Conference on Neural Information Processing Systems 2023, NeurIPS 2023, New Orleans, LA, USA, December 10 - 16, 2023*, 2023. 5

Huihui Gong, Minjing Dong, Siqi Ma, Seyit Camtepe, Surya Nepal, and Chang Xu. Stealthy Physical Masked Face Recognition Attack via Adversarial Style Optimization. *IEEE Trans. Multim.*, 26:5014–5025, 2024. 1, 2, 3, 4, 6, 7, 9, 10, 12, 23

Ian J. Goodfellow, Jonathon Shlens, and Christian Szegedy. Explaining and Harnessing Adversarial Examples. In *3rd International Conference on Learning Representations, ICLR 2015, San Diego, CA, USA, May 7-9, 2015, Conference Track Proceedings*, 2015. 5

Arthur Gretton, Karsten M. Borgwardt, Malte J. Rasch, Bernhard Schölkopf, and Alexander J. Smola. A Kernel Method for the Two-Sample-Problem. In Bernhard Schölkopf, John C. Platt, and Thomas Hofmann (eds.), *Advances in Neural Information Processing Systems 19, Proceedings of the Twentieth Annual Conference on Neural Information Processing Systems, Vancouver, British Columbia, Canada, December 4-7, 2006*, pp. 513–520. MIT Press, 2006. 13

Arthur Gretton, Karsten M. Borgwardt, Malte J. Rasch, Bernhard Schölkopf, and Alexander J. Smola. A Kernel Two-Sample Test. *J. Mach. Learn. Res.*, 13:723–773, 2012. 13

Chaoxiang He, Yimiao Zeng, Xiaojing Ma, Bin Benjamin Zhu, Zewei Li, Shixin Li, and Hai Jin. MysticMask: Adversarial Mask for Impersonation Attack Against Face Recognition Systems. In *IEEE International Conference on Multimedia and Expo, ICME 2024, Niagara Falls, ON, Canada, July 15-19, 2024*, pp. 1–6. IEEE, 2024. 12

Kaiming He, Xiangyu Zhang, Shaoqing Ren, and Jian Sun. Deep Residual Learning for Image Recognition. In *2016 IEEE Conference on Computer Vision and Pattern Recognition, CVPR 2016, Las Vegas, NV, USA, June 27-30, 2016*, pp. 770–778. IEEE Computer Society, 2016. 2

Martin Heusel, Hubert Ramsauer, Thomas Unterthiner, Bernhard Nessler, and Sepp Hochreiter. GANs Trained by a Two Time-Scale Update Rule Converge to a Local Nash Equilibrium. In Isabelle Guyon, Ulrike von Luxburg, Samy Bengio, Hanna M. Wallach, Rob Fergus, S. V. N. Vishwanathan, and Roman

Garnett (eds.), *Advances in Neural Information Processing Systems 30: Annual Conference on Neural Information Processing Systems 2017, December 4-9, 2017, Long Beach, CA, USA*, pp. 6626–6637, 2017. 12, 23

Jonathan Ho and Tim Salimans. Classifier-Free Diffusion Guidance. *CoRR*, abs/2207.12598, 2022. 4

Sadeep Jayasumana, Srikumar Ramalingam, Andreas Veit, Daniel Glasner, Ayan Chakrabarti, and Sanjiv Kumar. Rethinking FID: Towards a Better Evaluation Metric for Image Generation. In *IEEE/CVF Conference on Computer Vision and Pattern Recognition, CVPR 2024, Seattle, WA, USA, June 16-22, 2024*, pp. 9307–9315. IEEE, 2024. 8, 13

Caixin Kang, Yinpeng Dong, Zhengyi Wang, Shouwei Ruan, Hang Su, and Xingxing Wei. DIFFender: Diffusion-Based Adversarial Defense against Patch Attacks in the Physical World. *CoRR*, abs/2306.09124, 2023. 22

Tero Karras, Samuli Laine, and Timo Aila. A Style-Based Generator Architecture for Generative Adversarial Networks. In *IEEE Conference on Computer Vision and Pattern Recognition, CVPR 2019, Long Beach, CA, USA, June 16-20, 2019*, pp. 4401–4410. Computer Vision Foundation / IEEE, 2019. 8

Diederik P. Kingma and Jimmy Ba. Adam: A Method for Stochastic Optimization. In Yoshua Bengio and Yann LeCun (eds.), *3rd International Conference on Learning Representations, ICLR 2015, San Diego, CA, USA, May 7-9, 2015, Conference Track Proceedings*, 2015. 6

Stepan Komkov and Aleksandr Petiushko. AdvHat: Real-World Adversarial Attack on ArcFace Face ID System. In *2020 25th International Conference on Pattern Recognition (ICPR)*. IEEE, jan 2021. 1, 2, 7, 10, 12, 23

Akhil Kumar, Manisha Kaushal, and Akashdeep Sharma. SAM C-GAN: a method for removal of face masks from masked faces. *Signal Image Video Process.*, 17(7):3749–3757, 2023. 22

N. Kumar, A. C. Berg, P. N. Belhumeur, and S. K. Nayar. Attribute and Simile Classifiers for Face Verification. In *IEEE International Conference on Computer Vision (ICCV)*, Oct 2009. 2, 6, 9

Haoliang Li, Yufei Wang, Xiaofei Xie, Yang Liu, Shiqi Wang, Renjie Wan, Lap-Pui Chau, and Alex C. Kot. Light Can Hack Your Face! Black-box Backdoor Attack on Face Recognition Systems. *CoRR*, abs/2009.06996, 2020. 23

Jin Li, Ziqiang He, Anwei Luo, Jian-Fang Hu, Z. Jane Wang, and Xiangui Kang. AdvAD: Exploring Non-Parametric Diffusion for Imperceptible Adversarial Attacks. In *The Thirty-Eighth Annual Conference on Neural Information Processing Systems*, 2024. 22

Zaitang Li, Pin-Yu Chen, and Tsung-Yi Ho. GREAT Score: Global Robustness Evaluation of Adversarial Perturbation using generative models. *CoRR*, abs/2304.09875, 2023. 10

Chih-Yang Lin, Feng-Jie Chen, Hui-Fuang Ng, and Wei-Yang Lin. Invisible Adversarial Attacks on Deep Learning-Based Face Recognition Models. *IEEE Access*, 11:51567–51577, 2023. 1

Weiyang Liu, Yandong Wen, Zhiding Yu, Ming Li, Bhiksha Raj, and Le Song. SphereFace: Deep Hypersphere Embedding for Face Recognition. In *2017 IEEE Conference on Computer Vision and Pattern Recognition, CVPR 2017, Honolulu, HI, USA, July 21-26, 2017*, pp. 6738–6746. IEEE Computer Society, 2017. 22

Aleksander Madry, Aleksandar Makelov, Ludwig Schmidt, Dimitris Tsipras, and Adrian Vladu. Towards Deep Learning Models Resistant to Adversarial Attacks. In *6th International Conference on Learning Representations, ICLR 2018, Vancouver, BC, Canada, April 30 - May 3, 2018, Conference Track Proceedings*, 2018. 5, 22

Aravindh Mahendran and Andrea Vedaldi. Understanding deep image representations by inverting them. In *IEEE Conference on Computer Vision and Pattern Recognition, CVPR 2015, Boston, MA, USA, June 7-12, 2015*, pp. 5188–5196. IEEE Computer Society, 2015. 2

Dinh-Luan Nguyen, Sunpreet S. Arora, Yuhang Wu, and Hao Yang. Adversarial Light Projection Attacks on Face Recognition Systems: A Feasibility Study. In *2020 IEEE/CVF Conference on Computer Vision and Pattern Recognition, CVPR Workshops 2020, Seattle, WA, USA, June 14-19, 2020*, pp. 3548–3556. Computer Vision Foundation / IEEE, 2020. 23

Weili Nie, Brandon Guo, Yujia Huang, Chaowei Xiao, Arash Vahdat, and Animashree Anandkumar. Diffusion Models for Adversarial Purification. In Kamalika Chaudhuri, Stefanie Jegelka, Le Song, Csaba Szepesvári, Gang Niu, and Sivan Sabato (eds.), *International Conference on Machine Learning, ICML 2022, 17-23 July 2022, Baltimore, Maryland, USA*, volume 162 of *Proceedings of Machine Learning Research*, pp. 16805–16827. PMLR, 2022. 22

Mikhail Pautov, Grigorii Melnikov, Edgar Kaziakhmedov, Klim Kireev, and Aleksandr Petiushko. On adversarial patches: real-world attack on ArcFace-100 face recognition system. *CoRR*, abs/1910.07067, 2019. 1, 10, 12, 23

Alec Radford, Jong Wook Kim, Chris Hallacy, Aditya Ramesh, Gabriel Goh, Sandhini Agarwal, Girish Sastry, Amanda Askell, Pamela Mishkin, Jack Clark, Gretchen Krueger, and Ilya Sutskever. Learning Transferable Visual Models From Natural Language Supervision. In Marina Meila and Tong Zhang (eds.), *Proceedings of the 38th International Conference on Machine Learning, ICML 2021, 18-24 July 2021, Virtual Event*, volume 139 of *Proceedings of Machine Learning Research*, pp. 8748–8763. PMLR, 2021. 13

Robin Rombach, Andreas Blattmann, Dominik Lorenz, Patrick Esser, and Björn Ommer. High-Resolution Image Synthesis with Latent Diffusion Models. In *IEEE/CVF Conference on Computer Vision and Pattern Recognition, CVPR 2022, New Orleans, LA, USA, June 18-24, 2022*, pp. 10674–10685. IEEE, 2022. 3, 8

Quentin Le Roux, Eric Bourbao, Yannick Teglia, and Kassem Kallas. A Comprehensive Survey on Backdoor Attacks and Their Defenses in Face Recognition Systems. *IEEE Access*, 12:47433–47468, 2024. 23

Chitwan Saharia, William Chan, Saurabh Saxena, Lala Li, Jay Whang, Emily L. Denton, Seyed Kamyar Seyed Ghasemipour, Raphael Gontijo Lopes, Burcu Karagol Ayan, Tim Salimans, Jonathan Ho, David J. Fleet, and Mohammad Norouzi. Photorealistic Text-to-Image Diffusion Models with Deep Language Understanding. In *Advances in Neural Information Processing Systems 35: Annual Conference on Neural Information Processing Systems 2022, NeurIPS 2022, New Orleans, LA, USA, November 28 - December 9, 2022*, 2022. 24

Florian Schroff, Dmitry Kalenichenko, and James Philbin. FaceNet: A unified embedding for face recognition and clustering. In *IEEE Conference on Computer Vision and Pattern Recognition, CVPR 2015, Boston, MA, USA, June 7-12, 2015*, pp. 815–823. IEEE Computer Society, 2015. 22

Mahmood Sharif, Sruti Bhagavatula, Lujo Bauer, and Michael K. Reiter. A General Framework for Adversarial Examples with Objectives. *ACM Trans. Priv. Secur.*, 22(3):16:1–16:30, 2019. 1, 12, 13, 23, 28

Meng Shen, Zelin Liao, Liehuang Zhu, Ke Xu, and Xiaojiang Du. VLA: A Practical Visible Light-based Attack on Face Recognition Systems in Physical World. *Proc. ACM Interact. Mob. Wearable Ubiquitous Technol.*, 3(3):103:1–103:19, 2019. 23

Jiaming Song, Chenlin Meng, and Stefano Ermon. Denoising Diffusion Implicit Models. In *9th International Conference on Learning Representations, ICLR 2021, Virtual Event, Austria, May 3-7, 2021*. OpenReview.net, 2021. 5

Yang Song, Rui Shu, Nate Kushman, and Stefano Ermon. Constructing Unrestricted Adversarial Examples with Generative Models. In *Advances in Neural Information Processing Systems 31: Annual Conference on Neural Information Processing Systems 2018, NeurIPS 2018, December 3-8, 2018, Montréal, Canada*, pp. 8322–8333, 2018. 2, 22

Yuhao Sun, Lingyun Yu, Hongtao Xie, Jiaming Li, and Yongdong Zhang. DiffAM: Diffusion-Based Adversarial Makeup Transfer for Facial Privacy Protection. In *IEEE/CVF Conference on Computer Vision and*

Pattern Recognition, CVPR 2024, Seattle, WA, USA, June 16-22, 2024, pp. 24584–24594. IEEE, 2024. 1, 2, 7, 12, 23

Anjali T and Masilamani V. Text-Guided Synthesis of Masked Face Images. *ACM Transactions on Multimedia Computing, Communications, and Applications*, 21(1), 2024. ISSN 1551-6857. 22

Fatemeh Vakhshiteh, Ahmad Nickabadi, and Raghavendra Ramachandra. Adversarial Attacks Against Face Recognition: A Comprehensive Study. *IEEE Access*, 9:92735–92756, 2021. doi: 10.1109/ACCESS.2021.3092646. 1, 3, 6, 10

Hao Wang, Yitong Wang, Zheng Zhou, Xing Ji, Dihong Gong, Jingchao Zhou, Zhifeng Li, and Wei Liu. CosFace: Large Margin Cosine Loss for Deep Face Recognition. In *2018 IEEE Conference on Computer Vision and Pattern Recognition, CVPR 2018, Salt Lake City, UT, USA, June 18-22, 2018*, pp. 5265–5274. Computer Vision Foundation / IEEE Computer Society, 2018. 22

Zhongyuan Wang, Baojin Huang, Guangcheng Wang, Peng Yi, and Kui Jiang. Masked Face Recognition Dataset and Application. *IEEE Trans. Biom. Behav. Identity Sci.*, 5(2):298–304, 2023. 22

Zhou Wang, Alan C. Bovik, Hamid R. Sheikh, and Eero P. Simoncelli. Image quality assessment: from error visibility to structural similarity. *IEEE Trans. Image Process.*, 13(4):600–612, 2004. 12, 23

Yandong Wen, Kaipeng Zhang, Zhifeng Li, and Yu Qiao. A Discriminative Feature Learning Approach for Deep Face Recognition. In Bastian Leibe, Jiri Matas, Nicu Sebe, and Max Welling (eds.), *Computer Vision - ECCV 2016 - 14th European Conference, Amsterdam, The Netherlands, October 11-14, 2016, Proceedings, Part VII*, volume 9911 of *Lecture Notes in Computer Science*, pp. 499–515. Springer, 2016. 3, 22

Zihao Xiao, Xianfeng Gao, Chilin Fu, Yinpeng Dong, Wei Gao, Xiaolu Zhang, Jun Zhou, and Jun Zhu. Improving Transferability of Adversarial Patches on Face Recognition With Generative Models. In *IEEE Conference on Computer Vision and Pattern Recognition, CVPR 2021, virtual, June 19-25, 2021*, pp. 11845–11854. Computer Vision Foundation / IEEE, 2021. 1, 12

Tianxin Xie, Hu Han, Shiguang Shan, and Xilin Chen. Natural Adversarial Mask for Face Identity Protection in Physical World. *IEEE Transactions on Pattern Analysis and Machine Intelligence*, 47(3):2089–2106, 2025. 12

Haotian Xue, Alexandre Araujo, Bin Hu, and Yongxin Chen. Diffusion-Based Adversarial Sample Generation for Improved Stealthiness and Controllability. In Alice Oh, Tristan Naumann, Amir Globerson, Kate Saenko, Moritz Hardt, and Sergey Levine (eds.), *Advances in Neural Information Processing Systems 36: Annual Conference on Neural Information Processing Systems 2023, NeurIPS 2023, New Orleans, LA, USA, December 10 - 16, 2023*, 2023. 2, 22

Xiao Yang, Chang Liu, Longlong Xu, Yikai Wang, Yinpeng Dong, Ning Chen, Hang Su, and Jun Zhu. Towards Effective Adversarial Textured 3D Meshes on Physical Face Recognition. In *IEEE/CVF Conference on Computer Vision and Pattern Recognition, CVPR 2023, Vancouver, BC, Canada, June 17-24, 2023*, pp. 4119–4128. IEEE, 2023. 12

Bangjie Yin, Wenxuan Wang, Taiping Yao, Junfeng Guo, Zelun Kong, Shouhong Ding, Jilin Li, and Cong Liu. Adv-Makeup: A New Imperceptible and Transferable Attack on Face Recognition. In *Proceedings of the Thirtieth International Joint Conference on Artificial Intelligence, IJCAI 2021, Virtual Event / Montreal, Canada, 19-27 August 2021*, pp. 1252–1258. ijcai.org, 2021. 1, 7, 22

Shuai Yuan, Hongwei Li, Rui Zhang, Hangcheng Cao, Wenbo Jiang, Tao Ni, Wenshu Fan, Qingchuan Zhao, and Guowen Xu. Omni-Angle Assault: An Invisible and Powerful Physical Adversarial Attack on Face Recognition. In *Forty-second International Conference on Machine Learning (ICML)*, 2025. 23

Irad Zehavi and Adi Shamir. Facial Misrecognition Systems: Simple Weight Manipulations Force DNNs to Err Only on Specific Persons. *CoRR*, abs/2301.03118, 2023. 23

Kaipeng Zhang, Zhanpeng Zhang, Zhifeng Li, and Yu Qiao. Joint Face Detection and Alignment Using Multitask Cascaded Convolutional Networks. *IEEE Signal Process. Lett.*, 23(10):1499–1503, 2016. 8

Yinglin Zheng, Hao Yang, Ting Zhang, Jianmin Bao, Dongdong Chen, Yangyu Huang, Lu Yuan, Dong Chen, Ming Zeng, and Fang Wen. General Facial Representation Learning in a Visual-Linguistic Manner. In *IEEE/CVF Conference on Computer Vision and Pattern Recognition, CVPR 2022, New Orleans, LA, USA, June 18-24, 2022*, pp. 18676–18688. IEEE, 2022. 7

Zheng Zhu, Guan Huang, Jiankang Deng, Yun Ye, Junjie Huang, Xinze Chen, Jiagang Zhu, Tian Yang, Jia Guo, Jiwen Lu, Dalong Du, and Jie Zhou. Masked Face Recognition Challenge: The WebFace260M Track Report. *CoRR*, abs/2108.07189, 2021. 22

Alon Zolfi, Shai Avidan, Yuval Elovici, and Asaf Shabtai. Adversarial Mask: Real-World Universal Adversarial Attack on FaceRecognition Models. In Massih-Reza Amini, Stéphane Canu, Asja Fischer, Tias Guns, Petra Kralj Novak, and Grigorios Tsoumakas (eds.), *Machine Learning and Knowledge Discovery in Databases - European Conference,ECML PKDD 2022, Grenoble, France, September 19-23, 2022, Proceedings, Part III*, volume 13715 of *Lecture Notes in Computer Science*, pp. 304–320. Springer, 2022. 1, 2, 3, 4, 6, 7, 8, 10, 12, 23

A Extended Related Works

Facial Recognition: Facial recognition systems have evolved significantly over the last couple of decades, with the state of the art approaches using deep learning models that are able to achieve high accuracy in both large and small class sizes. Traditionally, for a small number of classes in a closed-set environment (that is the test set consists only of identities from within the training set), softmax-based approaches that are used in general object recognition can be effective. However, softmax losses encourage the learned features to be separable, but not necessarily discriminative (Wen et al., 2016), leading to worse performance when there are lots of classes of data or in an open-set environment, where the test set includes identities not in the training set (Liu et al., 2017).

Focus has moved to using Siamese networks (Bromley et al., 1993) where the backbone learns a discriminative, rather than separable, embedding space through different losses such as center loss (Wen et al., 2016) or triplet loss (Schroff et al., 2015). More recent work has focused on maximizing the angular margins of learnt class centers in a learnt embedding space, such that embeddings from a given class' center point are in a similar direction and that embeddings not from that center's class, point in a different direction (Liu et al., 2017). Several works have aimed for intra-class compactness and inter-class discrepancy with the aim of learning a discriminative embedding space (Liu et al., 2017; Wang et al., 2018; Deng et al., 2019a).

Masked face recognition has become of interest over the last several years (Zhu et al., 2021); with the challenge being to have a network that is effective for faces with and without a face mask on. This has led to datasets of masked faces for which there are now several including real and synthetic datasets (Wang et al., 2023; Anjali & Masilamani, 2024).

Adversarial Examples using Generative Models: Traditionally, adversarial examples were generated using gradient based methods such that the perturbation has a small matrix norm; one example is using projected gradient descent (PGD) (Madry et al., 2018). However, Song et al. (2018) used generative models (specifically generative adversarial networks) to construct unrestricted adversarial examples that exhibit greater realism. This has progressed so that recently there have been several works proposing diffusion model based adversarial attacks using different techniques (Xue et al., 2023; Chen et al., 2023; Dai et al., 2024). Using diffusion models for this task has several benefits, most notably, greater controllability and visual fidelity of generated samples (Dai et al., 2024), areas in which previous adversarial accessories struggled. Our attack, therefore, leverages these properties through the use of a textually controlled diffusion model. Nevertheless, finding imperceptible potent adversarial examples for accessories is difficult, however recently (Li et al., 2024) has proposed an alternative non parametric approach to adversarial example generation which could be a promising direction for future accessories to explore.

Patch-based Adversarial Attacks and Defenses: Adversarial patches (Brown et al., 2017) are small patterns that when placed within an input image, cause unintentional behavior in a network. To improve the robustness of these patches to real world conditions, past work has shown that it is necessary to incorporate real world transformations into the generation process (Athalye et al., 2018). In the context of adversarial accessories, this translates to generating on different images of a person, for example at different poses, such that different transformations are considered during accessory generation.

From the perspective of defending adversarial attacks, recent defenses have utilized diffusion models (Nie et al., 2022) for purification of adversarial examples, removing the perturbation while maintaining the original content. For adversarial patches, these techniques have been found to be inadequate, therefore, specific adversarial patch defenses have been developed (Kang et al., 2023). These defenses use diffusion models to locate the patch and then replace it using inpainting, which could be used to replace a face mask with an estimated face. Another defense would be to remove face masks from images using generative models trained to do so (Kumar et al., 2023). All current adversarial face masks are vulnerable to these last two defenses and so creating robustness to these defenses is not within the scope of our work and could be the goal of future work.

Other Attacks on Facial Recognition: There have also been other attacks on these systems such as adversarial makeup (Yin et al., 2021) which has been used so that the attack can access a wider area of the

face rather than just a local patch. Recent work has used diffusion models to enhance this approach further (Sun et al., 2024) creating highly realistic makeup to fool these models. These attacks have a significantly larger area of the face to attack and may be difficult to physically realize compared to face masks.

Another channel of attack is using visible light (Shen et al., 2019; Nguyen et al., 2020; Li et al., 2020) where perturbations are projected onto the face. These attacks offer a different representation to their perturbations which presents unique challenges which could also be explored with diffusion models in a similar fashion to our work. More recent work have developed adversarial props that emit adversarially crafted ultraviolet light for a variety of adversarial objectives which has the advantage of not being visible to the naked eye (Yuan et al., 2025).

Backdoor attacks on face recognition have also been developed, where the system behaves as expected on clean input but then has been modified to behave erroneously on malicious input. These attacks can be split into three components: the attack channel (the attacker's knowledge and access to the victim model), the injection method (how the manipulation can occur) and the trigger method (what triggers the corruption) (Roux et al., 2024). One such example work has directly manipulated weights such that only certain identities are misclassified, but the rest are unaffected (Zehavi & Shamir, 2023).

Another type of attack are those that poison the training set of a victim model such that when the attacker wears a physical accessory, the model erroneously classifies them (Chen et al., 2017).

These methods have a different threat model to our work, but are a different avenue of work that could be expanded using diffusion models.

B Evaluating Styles

Previous Style Metrics: As previously discussed, most adversarial accessory work has not focused on stealth and so there is a limited range of quantitative measures for stealthiness. Previous work has used TV loss to ensure accessories are color smooth, making them easier to physically realize and less noise like, but often stealthiness is not explicitly measured after generation (Zolfi et al., 2022; Komkov & Petiushko, 2021; Pautov et al., 2019).

Stealthiness is a subjective measure so an ideal method would be to collect user surveys, as has been done before (Sharif et al., 2019) where participants were asked to identity whether given images of glasses were "real" or generated. While this does gather valuable user opinion, these surveys are time consuming to run, potentially hard to reproduce when ran on a small scale and may not accurately measure stealthiness (as the concept is abstract to the general public). Some measures that have been used before in makeup attacks (Sun et al., 2024) are SSIM (Wang et al., 2004), PSNR and FID (Heusel et al., 2017). In recent stealthy mask work, Gong et al. (2024) measure the SSIM of masked faces with the mask texture being the original pattern in the style of their adversarial pattern and then comparing these images to masked faces with the adversarial pattern. Whilst these measures are able to yield valuable statistics about a generated accessory, we believe these do not capture the true essence of stealthiness – a better metric would be one which determines the quality of generated images. This can be achieved by treating the adversarial attack as an image generator and using similar metrics to measure its performance such as CMMD.

Proper Use of CMMD: When choosing images for CMMD evaluation for general accessory evaluation in future work, we recommend trying to evaluate on as close of a representation as the texture in the final accessory while avoiding any faces being in the images (such as the images in figure 5). Furthermore, the reference set for the style should be one image representing the style the textures in the generated set are attempting to create. The generated set should contain multiple textures from different attacks (i.e different attackers/targets) of the same style.

C Testing Different Styles and Text Prompts

Section 3 focused on two styles that were chosen due to being effective for the adversarial mask generation. However, to demonstrate the effectiveness of the stealth based approaches on a wide range of styles we test

Attack	Style	SR 100 (↑)	SR 1000 (↑)	Mask CMMD (↓)
SASMask-b	*Blue Dog*	1.0000	1.0000	5.2105
DAFR-d		1.0000	1.0000	2.0459
SASMask-b	*Panda Emoji*	1.0000	1.0000	3.0371
DAFR-d		1.0000	1.0000	0.8545
SASMask-b	*Black Sandwich*	1.0000	1.0000	4.9492
DAFR-d		1.0000	1.0000	2.7075
SASMask-b	*Owl*	1.0000	1.0000	5.5044
DAFR-d		1.0000	1.0000	1.2581
SASMask-b	*Giraffe*	1.0000	1.0000	1.8137
DAFR-d		1.0000	1.0000	0.7100
SASMask-b	*Bricks*	1.0000	1.0000	3.5112
DAFR-d		1.0000	1.0000	1.3195
SASMask-b	***Overall***	1.0000	1.0000	4.1125
DAFR-d		0.9930	0.9970	1.5663

Table 5: Some of the results from the style attack test on MobileFaceNet, for 6 out of the 20 styles chosen from filtered DrawBench. These tests use the same metrics as table 3, so a larger success rate (SR 100 and SR 1000) is desirable.

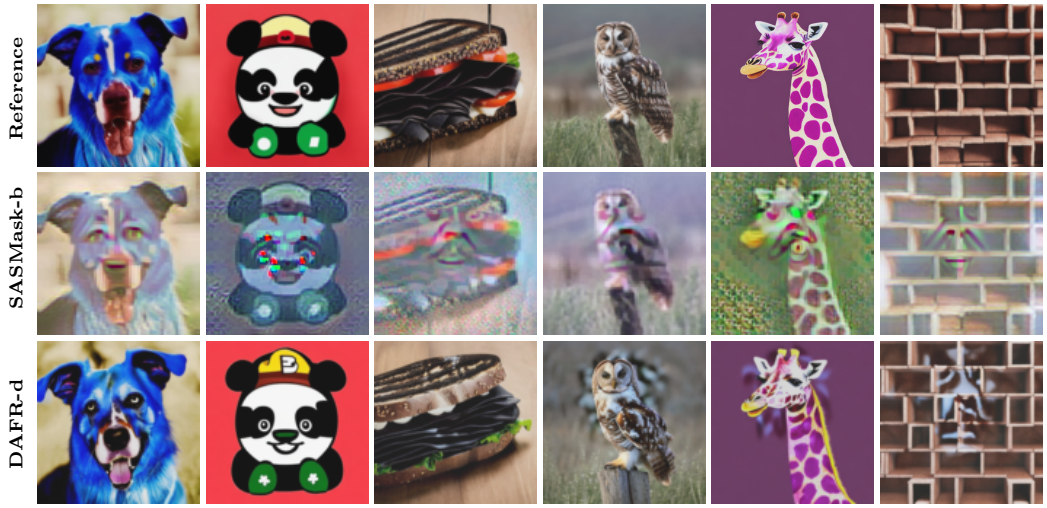

Figure 9: Textures from masks trying to dodge from the "Kiera Knightley" identity from the style test. The top row is reference images, the next row is generated by **SASMask-b** and the final row is generated by **DAFR-d**.

both DAFR and SASMask on 20 randomly chosen text prompts from a filtered set of DrawBench prompts (Saharia et al., 2022). Stealthy approaches may try to "hide" their perturbations in the content making more abstract content better as the content can vary significantly while still being faithful. Prompts from DrawBench are more concrete and contain a wide range of content, and test whether these attacks can still be stealthy even when not given an advantageous style. The same dodging benchmark was used as has been used in section 3, but 5 identities were chosen out of the previous 30 with the same number of images used for generation and testing as used previously.

Table 5 shows the results of our test on MobileFaceNet. Both attacks are successfully able to fool the network consistently, however DAFR generates stealthier masks as demonstrated by CMMD and by the visual results shown in figure 9. DAFR can achieve adversarial strength by manipulating the content of the textures in a manner faithful to the style, such as changing the hat, eyes and mouth of the panda in figure 9.

Attack	Arch.	Style	Cosine (↓)	M-CMMD (↓)
SASMask-d	R100	*Blue Dog*	0.1206	5.4339
DAFR-b			0.1718	2.4962
SASMask-d	R100	*Panda Emoji*	0.1036	5.0528
DAFR-b			0.2090	3.7732
SASMask-d	R100	*Black Sandwich*	0.0666	4.9142
DAFR-b			0.1766	2.9478
SASMask-d	R100	*Owl*	0.1092	7.1989
DAFR-b			0.1769	5.4135
SASMask-d	R100	*Giraffe*	0.0967	3.5704
DAFR-b			0.2049	1.5187
SASMask-d	R100	*Bricks*	0.0960	4.5317
DAFR-b			0.1636	2.5308
SASMask-d	R100	***Overall***	0.1238	4.9267
DAFR-b			0.1742	2.8558
SASMask-d	FT100	*Blue Dog*	0.2052	6.0991
DAFR-b			0.1367	3.2306
SASMask-d	FT100	*Panda Emoji*	0.1497	5.3878
DAFR-b			0.2076	4.4728
SASMask-d	FT100	*Black Sandwich*	0.4963	5.2030
DAFR-b			0.1633	2.5514
SASMask-d	FT100	*Owl*	0.3402	6.0632
DAFR-b			0.3065	3.5993
SASMask-d	FT100	*Giraffe*	0.3718	4.3375
DAFR-b			0.2734	2.0177
SASMask-d	FT100	*Bricks*	0.2779	3.9697
DAFR-b			0.1917	2.7599
SASMask-d	FT100	***Overall***	0.3497	4.8297
DAFR-b			0.1718	2.6770

Table 6: Results from the style attack test using 6 out of the 20 styles chosen from filtered DrawBench. Cosine is the mean cosine, while M-CMMD is the masked texture CMMD from table 3.

We conduct the same study as performed on MobileFaceNet, but using FT100 and R100. The attacks were less successful against these networks (refer to table 3) so these tests demonstrate the attacks ability to remain stealthy in a more difficult scenario.

Table 6 and figure 10 display selected results and textures from the style test on FT100 and R100. Firstly, DAFR outperformed SASMask on these obscure styles both stylewise and adversarially on FT100, while performing slightly worse adversarially on R100. Both attacks have significantly higher mask CMMD values compared to the tests with an advantageous style in previous sections. While an attacker can always choose to use an advantageous style, future work should focus on making an attack that can work on a wider range of styles.

D Testing Different Face Poses

An advantage of using FAAB is that a deeper understanding of the different properties of an accessory is evaluated such as its robustness to different face poses, with figure 6 demonstrating the variety of poses. We now analyze the effectiveness of the different face mask attacks when they are used at different angles. To measure the pose of each face, the yaw, pitch and roll are calculated, allowing the images to be classified into two categories: straight on and angled. Straight on images represented around 67% of the images while angled represented 31% of the images with the remaining 2% representing images with an extreme yaw and patch.

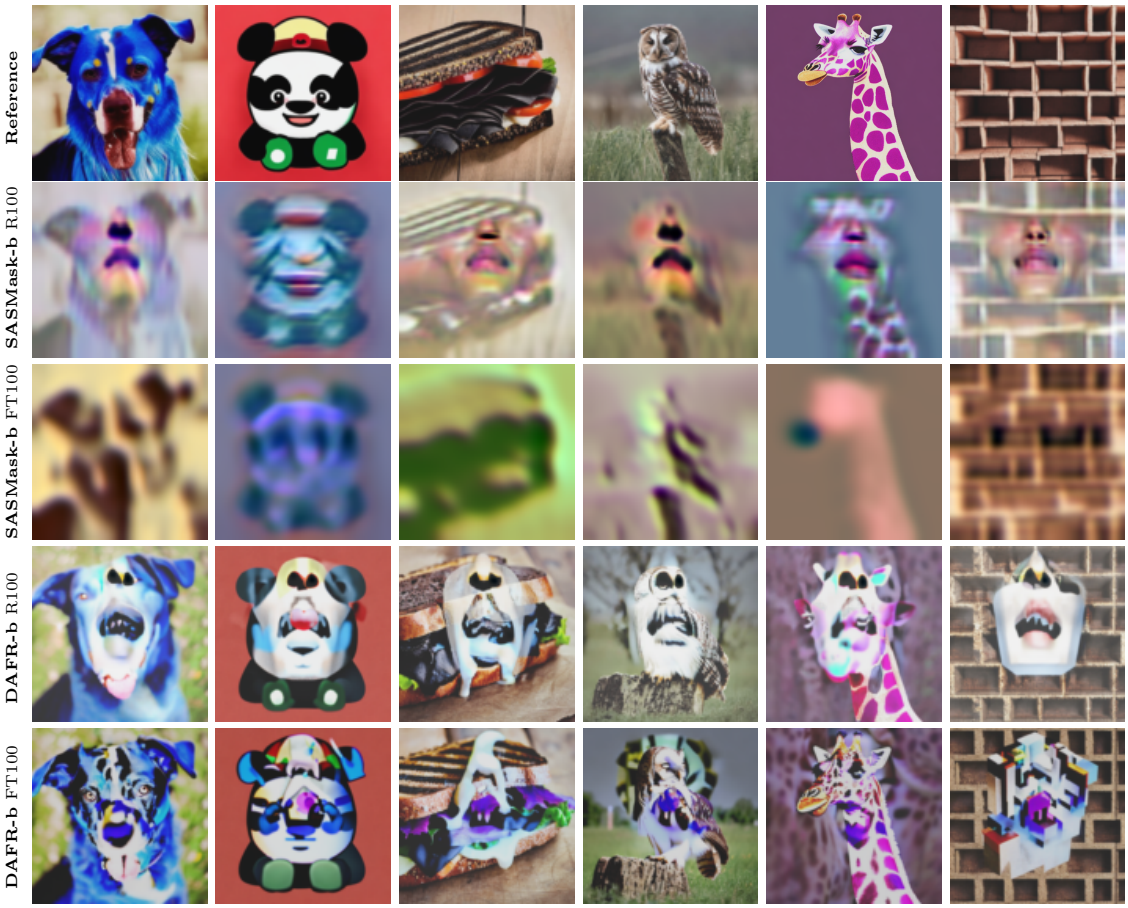

Figure 10: Textures from masks trying to dodge from the "Kiera Knightley" identity from the style test. The content of the rows from top to bottom are reference images, **SASMask-d** R100, **SASMask-d** FT100, **DAFR-b** R100, **DAFR-b** FT100

1. Straight on images have the magnitudes of yaw and pitch less than 15 degrees.
2. Angled images have either their yaw or pitch with a magnitude greater than 15 degrees while still both having a magnitude less than 45 degrees.

Table 7 shows the efficacy of the different masks when tested on different angles. It is important to notice that all the non adversarial masks become more effective when the attacker is at an angle compared to being straight on. However, when it comes to DAFR face masks, the performance tends to increase as well (such as on R100 and FaRL), which may occur due to the benefit of less of the face being in the image. When masks have a high efficacy such as DAFR in FT100 and AdvMask and SASMask in R100, the negative effect of having less of the adversarial texture in the image may outweigh the effect of having less of the face in the image. This suggests that DAFR has similar robustness to other masks generated using multiple images during generation while maintaining more stealthiness.

E Testing Different Brightness

To test the robustness of the generated textures to different brightness conditions to test whether the accessory works in both dimly lit or brightly illuminated rooms. After a mask is applied to a given test image, the image is converted to the HSV color space where the value channel is randomly adjusted while ensuring

Architecture	Attack	Straight On		Angled	
		SR 100 (↑)	*SR 1000* (↑)	*SR 100* (↑)	*SR 1000* (↑)
FT100	**Non Adv.**	0.2650	0.6800	0.2979	0.7660
	AdvMask-b	**1.0000**	**1.0000**	**0.9787**	**1.0000**
	SASMask-d	0.5600	0.8100	0.5426	0.8191
	DAFR-b	*0.9250*	*0.9900*	*0.8830*	*0.9894*
R100	**Non Adv.**	0.0450	0.0450	0.0745	0.0745
	AdvMask-b	**0.9750**	**0.9650**	**0.9149**	**0.8830**
	SASMask-d	*0.9300*	*0.8800*	*0.8617*	*0.8298*
	DAFR-b	0.6550	0.5800	0.6915	0.5745
FaRL	**Non Adv.**	0.1850	0.1550	0.2021	0.1808
	AdvMask-b	**1.0000**	**1.0000**	**1.0000**	**1.0000**
	SASMask-d	**1.0000**	**1.0000**	**1.0000**	**1.0000**
	DAFR-b	*0.5100*	*0.4800*	*0.5851*	*0.5532*
MFN	**Non Adv.**	0.0725	0.1399	0.1275	0.3137
	AdvMask-b	**1.0000**	**1.0000**	**1.0000**	**1.0000**
	SASMask-b	**1.0000**	**1.0000**	**1.0000**	**1.0000**
	DAFR-d	*0.9378*	*0.9948*	*0.9804*	**1.0000**

Table 7: Results of the attacks at different angles. When the attack has a style, we show the blue flower pattern style. These results come from benchmarks from the earlier sections or identical reran benchmarks. For each column within the attacks on the same target network, a marker has been used to indicate rank: **1st**, *2nd* and 3rd.

Architecture	Attack	Brightness Variance		No Adjustments	
		SR 100 (↑)	*SR 1000* (↑)	*SR 100* (↑)	*SR 1000* (↑)
FT100	**Non Adv.**	0.2433	0.6900	0.2767	0.7133
	AdvMask-b	**0.9900**	**1.0000**	**0.9867**	**1.0000**
	SASMask-d	0.5267	0.8100	0.5533	0.8167
	DAFR-b	*0.9200*	*0.9867*	*0.9033*	0.9900
MFN	**Non Adv.**	0.0967	0.1767	0.1000	0.2100
	AdvMask-b	**1.0000**	**1.0000**	**1.0000**	**1.0000**
	SASMask-b	**1.0000**	**1.0000**	**1.0000**	**1.0000**
	DAFR-d	*0.9500*	*0.9867*	*0.9533*	*0.9967*
R100	**Non Adv.**	0.0767	0.0733	0.0733	0.0733
	AdvMask-b	**0.9800**	**0.9467**	**0.9567**	**0.9400**
	SASMask-d	*0.9167*	*0.8767*	*0.9100*	*0.8667*
	DAFR-b	0.7333	0.6367	0.6733	0.5867
FaRL	**Non Adv.**	0.1967	0.1833	0.2067	0.1800
	AdvMask-b	**1.0000**	**1.0000**	**1.0000**	**1.0000**
	SASMask-d	**1.0000**	**1.0000**	**1.0000**	**1.0000**
	DAFR-b	*0.5367*	*0.5200*	*0.5433*	*0.5133*

Table 8: Results of the attacks when the brightness of the image is randomly adjusted. When the attack has a style, we show the blue flower pattern style. The "No Adjustment" results come from the benchmarks from earlier sections. For each column within the attacks on the same target network, a marker has been used to indicate rank: **1st**, *2nd* and 3rd.

that the pixel values remain within a valid range. This has the effect of randomly changing the brightness of the images as demonstrated in figure 11.

Table 8 shows the results of some of the benchmarks used previously when tested with random brightness. Modifying brightness of the images can have a significant impact on the efficacy of these accessories, with this impact either potentially being positive or negative. In general, the attacks demonstrate similar levels of

Architecture	Attack	Match Lighting		No Adjustments	
		SR 100 (↑)	*SR 1000* (↑)	*SR 100* (↑)	*SR 1000* (↑)
FT100	**Non Adv.**	0.3200	0.7267	0.2767	0.7133
	AdvMask-b	**0.9133**	**0.9867**	**0.9867**	**1.0000**
	SASMask-d	0.5500	0.8133	0.5533	0.8167
	DAFR-b	*0.7333*	*0.9367*	*0.9033*	*0.9900*
MFN	**Non Adv.**	0.0967	0.1567	0.1000	0.2100
	AdvMask-b	*0.9333*	*0.9767*	**1.0000**	**1.0000**
	SASMask-b	**0.9967**	**0.9967**	**1.0000**	**1.0000**
	DAFR-d	0.8200	0.9467	0.9533	0.9967
R100	**Non Adv.**	0.0733	0.0733	0.0733	0.0733
	AdvMask-b	**0.8733**	**0.8233**	**0.9567**	**0.9400**
	SASMask-d	*0.8467*	*0.7600*	*0.9100*	*0.8667*
	DAFR-b	0.5033	0.4033	0.6733	0.5867
FaRL	**Non Adv.**	0.2400	0.2333	0.2067	0.1800
	AdvMask-b	**1.0000**	*0.9967*	**1.0000**	**1.0000**
	SASMask-d	**1.0000**	**1.0000**	**1.0000**	**1.0000**
	DAFR-b	*0.4600*	0.4433	*0.5433*	*0.5133*

Table 9: Results of the attacks when the lighting on the mask is adjusted to match the lighting of the rest of the image. When the attack has a style, we show the blue flower pattern style. The "No Adjustment" results come from the benchmarks from earlier sections. For each column within the attacks on the same target network, a marker has been used to indicate rank: **1st**, *2nd* and 3rd.

performance before and after the brightness changes suggesting these attacks all have robustness to different brightness conditions. For these masks to be robust to physical conditions they must be robust in a variety of different brightness conditions therefore it is encouraging that all the attacks demonstrate this robustness.

F Testing Different Lighting

One of the properties of the accessories we wanted to test is their robustness to different lighting conditions. Previous work (Sharif et al., 2019) has manipulate the luminance of the tested images to test their accessories for this robustness. We use manipulate the textures of the accessories to have a similar luminance to the test image, therefore testing these masks in a more realistic setting where their luminance matches the rest of the image, often making these masks darker and less radiant as shown in figure 12.

Table 9 shows the results of some of the benchmarks used previously when tested with adjusted lighting. Modifying the textures to have a more realistic luminance can have a significant negative impact on the efficacy of these accessories. DAFR generates adversarial textures to be stealthy however this may generate intricate patterns that are less robust to physical conditions not necessarily present during generation. This is important for physically realizing these masks thus testing in such a way is vital to ensure that results generalize from the digital to the physical domain. Future work in stealthy adversarial accessory generation should try to generate masks that are more robust to physical conditions while being stealthy.

G Statement of Broader Impact

Deep learning based facial recognition and verification systems are becoming more prominent around the world. On one hand, DAFR highlights new security risks to existing face recognition and verification systems by creating masks that are indistinguishable from more colorful masks people wear; which could undermine their efficacy and the trust put in them. However, by demonstrating these capabilities, future defenses and adversarial training schemes will have to consider these types of accessories thus allowing future work to defend against DAFR or a more advanced version of it. On the other hand, these powerful systems can be

misused by different institutions and the existence of these accessories demonstrate that these systems are not flawless and can be manipulated in certain circumstances.

H Reproducibility Statement

All the work for this project was performed on a single NVIDIA A5000 GPU. Depending on the attack type and hyperparameters, each benchmark could take between 40 minutes to 7 hours to generate all 30 different adversarial textures used for results in section 3. To evaluate the different metrics evaluated within these benchmarks on the GPU would require around 30 minutes. The main body contains 50 benchmarks which would take roughly 286 hours on a single GPU, with the appendix benchmarks taking a further 100 hours. The supplementary material contains all the code to run the work, including Python code for all the attacks, benchmark and other utilities (such as threshold selection etc.). Instructions have been provided to help run the code.

To reproduce the physical evaluation, the code provided will be sufficient. The masked textures generated by these methods were resized using cubic interpolation such that when printed out fit over the face in a similar fashion as the digitally placed masks. This may cause the mask to vary in size depending on the attacker. MTCNN alignment was effective at detecting faces with face masks, while FFHQ struggled so this should be taken into consideration when taking physical photos for evaluation.

Figure 11: The top row are images of "Drew Barrymore" from the PubFig dataset with a face mask digitally augmented on. The bottom row are the same images but after the brightness of the image has been randomly altered.

Figure 12: The top row are images of "Drew Barrymore" from the PubFig dataset with a face mask digitally augmented on. The bottom row are the same images but after the lighting of the face mask has been matched with the rest of the image.